Journal of Sedimentary Research

Journal of Sedimentary Research, 2023, v. 93, 145–160
Research Article
DOI: 10.2110/jsr.2022.066

ALWAYS A WHITE CHRISTMAS IN THE BAHAMAS: TEMPERATURE AND HYDRODYNAMICS LOCALIZE WINTER MUD PRODUCTION ON GREAT BAHAMA BANK

SAM J. PURKIS,[1] AMANDA M. OEHLERT,[1] THOMAS DOBBELAERE,[2] EMMANUEL HANERT,[2] AND PAUL (MITCH) HARRIS[1]
[1]CSL, Center for Carbonate Research, Department of Marine Geosciences, Rosenstiel School of Marine, Atmospheric, and Earth Science, University of Miami, Miami, Florida, 33149, U.S.A.
[2]Earth and Life Institute and Institute of Mechanics, Materials and Civil Engineering, Université Catholique de Louvain, Louvain-la-Neuve, Belgium
e-mail: spurkis@rsmas.miami.edu

ABSTRACT: **Whitings, or occurrences of fine-grained carbonate in the water column, have been observed in modern environments with salinities ranging from fresh to marine conditions, and thick deposits of lime mud are described throughout the geological record. Despite their ubiquity, the trigger for whitings has been debated for more than eighty years. Satellite data reveal that most whitings are restricted to the northwestern part of Great Bahama Bank (GBB) which occupies < 10% of the platform area. Even here, whitings are further focused. More than 35% of them occur in a zone which occupies just 1% of the platform. We propose a three-step process for the existence of this zone of peak whitings and why the whitings in it are both more frequent and larger in winter than summer. First, the temperature differential between on- and off-platform waters is highest in the winter, setting up a disparity between dissolved CO_2 concentrations in the two water masses. Second, hydrodynamic mixing of these two water masses increases the degree of aragonite saturation of the platform-top waters, as colder on-platform waters with theoretically higher concentrations of dissolved gases are warmed via mixing with the warmer off-platform waters. Finally, spatial heterogeneity in the degree of aragonite saturation is higher in the winter, and the zone of peak whitings is situated in an area of locally enhanced saturation state. Hydrodynamic simulation suggests that the whitings zone is located by tidal inflow of off-platform waters across the western margin of GBB, as well as inflow from the Tongue of the Ocean to the north of Andros Island. Despite thermodynamic forcing mechanisms that predict higher frequency of whitings in the summer, the environmental, hydrodynamic, geochemical, and kinetic conditions in the whitings zone appear to support the Goldilocks configuration that enhances the formation of wintertime whitings on Great Bahama Bank. This phenomenon has implications for the interpretation of whitings mud in the geological record, including the geochemical signatures within it.**

INTRODUCTION

The term "whiting" is used to describe occurrences of fine-grained carbonate, or lime mud, precipitated directly from both marine and fresh waters. Great Bahama Bank (Fig. 1) has become a common venue to study these enigmatic events and their causes. To the latter, a pair of hypotheses have risen to the fore, of which the first pins whitings mud to be resuspended from the seabed (Broecker and Takahashi 1966; Morse et al. 1984, 2003; Boss and Neumann 1993; Broecker et al. 2000; Dierssen et al. 2009). The second hypothesis ascribes whitings to originate from direct precipitation of carbonate from the water column, likely in association with cyanobacteria (Smith 1940; Shinn et al. 1989; Robbins and Blackwelder 1992; Robbins et al. 1997; Schultze-Lam et al. 1997; Thompson et al. 1997; Yates and Robbins 1998; Swart et al. 2014). Finally, a recent study proposed that abrasion of carbonate grains, such as ooids, can produce mud-size carbonate that could plausibly exhibit geochemical and physical characteristics similar to those of the enigmatic Great Bahama Bank (GBB) whitings (Trower et al. 2019).

Although marine whitings are relatively rare outside Floridian waters, the Bahamas, and the Persian/Arabian Gulf, there are at least two reasons why they have been studied for 80+ years. First, even though individual whitings are small, their collective ability to produce lime mud is staggering. For instance, Robbins et al. (1997) emphasized how whitings conceivably account for all the fine sediment residing on the 100,000 sq. km GBB—the largest carbonate platform on Earth—and plenty more besides. Whitings-produced mud atop GBB has been prolific at least since the Miocene (Turpin et al. 2011). The second reason that whitings have garnered attention is their relevance to producing and accumulating carbonates in deep geological time—before the evolution of the myriad of carbonate-secreting organisms, abiotic precipitation of aragonite might have been the dominant source of Earth's Proterozoic limestone edifices (Sandberg 1983, 1985; Knoll and Swett 1990; Hoffman et al. 1998; Riding 1991, 2006).

Our previous work (Purkis et al. 2017) emphasizes that more than 35% of all whitings atop GBB occur within a localized "peak whitings" zone that encompasses < 1% of the total area of the platform (Fig. 1). This observation suggests that, in this small area, environmental conditions uniquely favor enhanced formation of whitings. This paper builds forward from Purkis et al. (2017) in which we paired platform-wide observations of whitings on GBB with hydrodynamic modeling to explore their triggers. This paper is an evolution over our preceding work because it presents a

Published Online: March 2023
 1527-1404/23/093-145

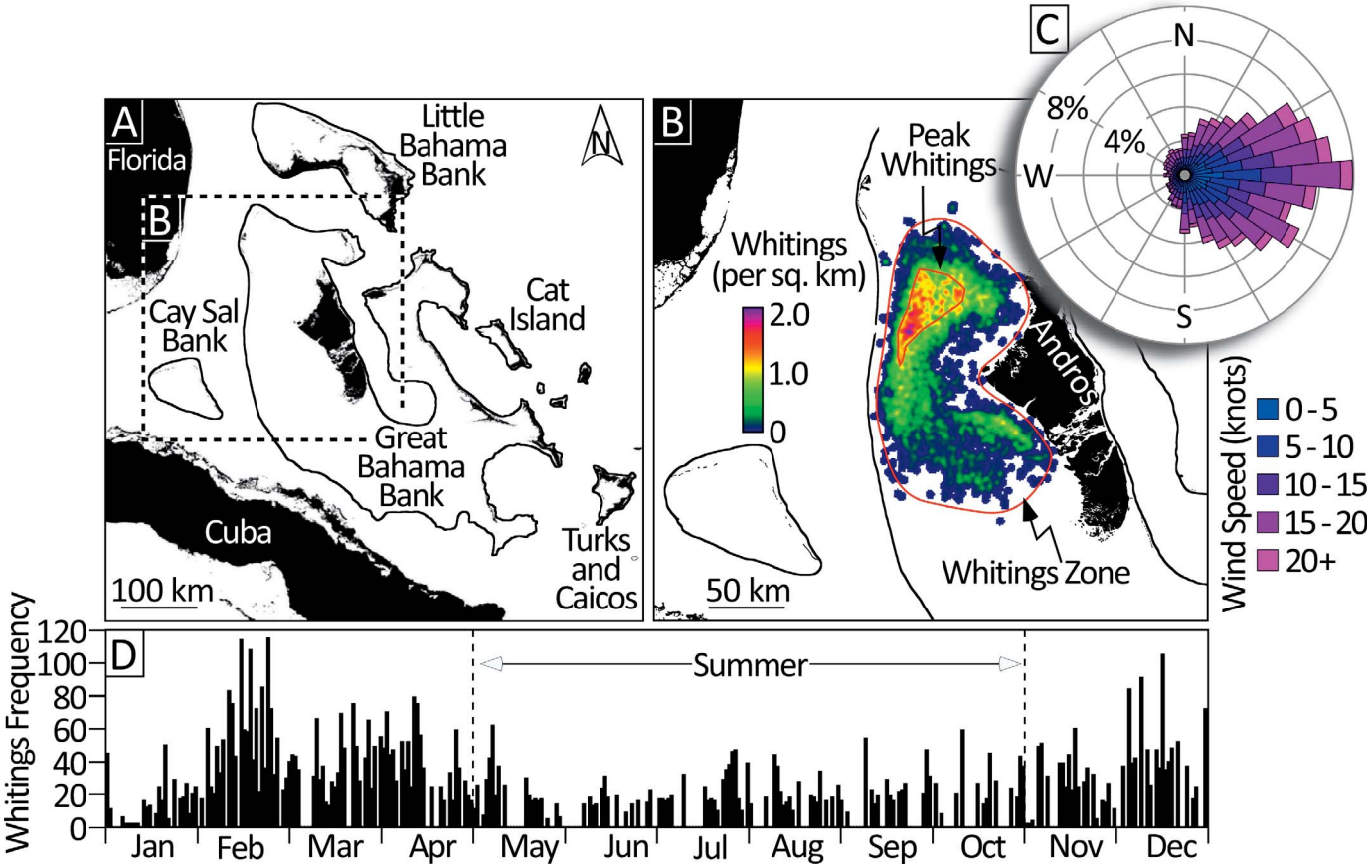

FIG. 1.—**A)** Depicts the scope for the SLIM hydrodynamic simulation which extends over a domain of 500,000 sq. km. Great Bahama Bank (GBB) is a 100,000 sq. km shallow-water carbonate platform situated east of Florida and north of Cuba. 60% of GBB lies in 5 m or less of water. **B)** Density of ~ 15,000 individual GBB whitings tallied from MODIS satellite imagery during 2012, 2014, and 2016. More than 35% of the observed precipitation events occur within the "Peak Whitings" polygon which covers an area of 1,000 sq. km (just 1% of the area of GBB), emphasizing that the spatial occurrence of whitings on this platform is non-random and geographically focused. **C)** Wind rose for GBB extracted from QuikSCAT observations for 2016. The platform is dominated by easterlies. **D)** Seasonality of whitings atop GBB (averaged over 2012, 2014, and 2016). Whitings in the winter (Nov–Apr) are 70% more numerous than in the summer (May–Oct).

new hydrodynamic simulation which is more than one order of magnitude higher in fidelity than previously published. Further, the new hydrodynamic simulation is used to drive a model of the spatial heterogeneity in aragonite saturation state atop GBB and to test whether the minimum velocity needed to loft fine-grained sediments is achieved, providing new insight into the resuspension hypothesis for the formation of whitings. In combination, we deploy these models to further examine whitings triggers. Our long-term goal is to better understand Holocene lime-mud production in the Bahamas as a modern analog to its occurrence in the geological record. This paper addresses that goal by pursuing three specific aims:

1. To track individual whitings through time using satellite imagery to audit their persistence, allowing the debate to be settled as to whether they owe themselves to resuspended bottom sediment or precipitation.
2. To generate an improved simulation of platform-top currents for the entirety of GBB and its surrounding waters. As developed by Purkis et al. (2017), we hypothesize that currents play a role in both initiating and spatially locating whitings.
3. To examine seasonal changes in the degree of aragonite saturation of platform-top waters driven by on- and off-platform temperature differentials as a modulator of carbonate precipitation rate and thus the seasonal frequency of whitings. We hypothesize that whitings are suppressed in the summer when the gradient in saturation state between on- and off-platform waters is minimized.

Counting Whitings from Orbit

Since we incorporate the whitings dataset developed by Purkis et al. (2017), the method of counting whitings will be treated only briefly here. As pioneered by Dierssen et al. (2009) and Yao et al. (2023), whitings can be reliably delineated using 250-m-resolution Moderate Resolution Imaging Spectroradiometer (MODIS) satellite data, a sensor which offers two overpasses per day. We examined 515 cloud-free MODIS images acquired in 2012 and 2014 and mapped the coordinates of the centroid of every recognizable whiting to determine their spatial and temporal distributions (Fig. 1). In addition to data presented by Purkis et al. (2017), we further digitized the boundaries of 2,270 whitings in 205 cloud-free MODIS images from 2016. These new data from 2016 have the advantage of reporting not only the frequency of the whitings and their locations, but also their areal extents. Whitings were differentiated from storm events on the MODIS imagery by size. As reported by Lopez-Gamundi et al. (2022), storm events like Hurricane Matthew which traversed GBB on October 5th–6th, 2016 generate large (> 500 sq. km) resuspension events that span the platform top. By comparison, individual whitings are tiny. Based on our 2016 dataset, the average size of a whiting is 15 sq. km. Statistical significance of differences between the means of both whitings frequency and latitudinal precinct (north vs. south) by season (summer vs. winter) was assessed using two-tailed Student's t-tests

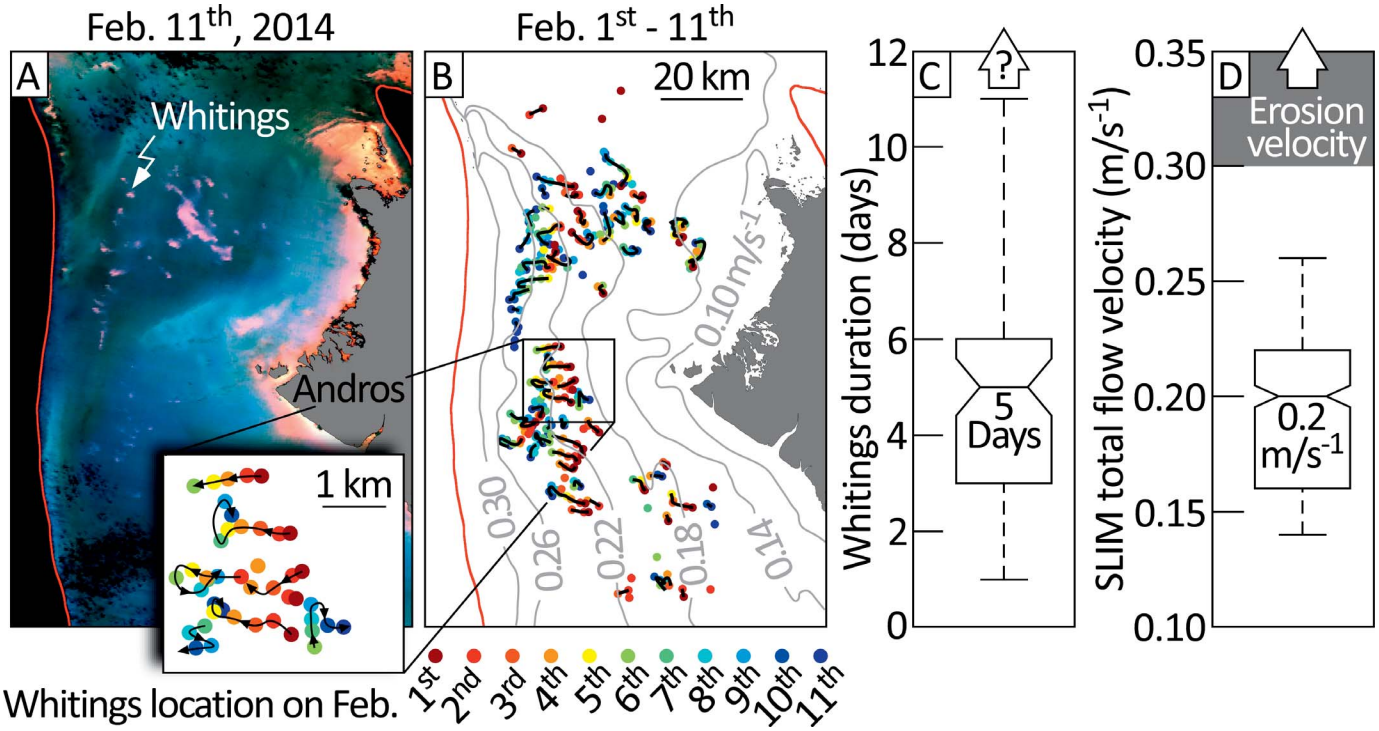

FIG. 2.—**A)** A population of whitings atop the Great Bahama Bank (GBB) imaged by the Moderate Resolution Imaging Spectroradiometer (MODIS) on February 11th, 2014. Whitings are expressed in the imagery as a white discoloration to the water column. **B)** Tracks the movement of the population of 166 whitings active atop GBB from Feb. 1st through 14th, 2014, using successive MODIS overpasses across 11 consecutive cloud-free days. Contour lines depict total current speeds predicted by the SLIM hydrodynamic model averaged over these days. **C)** Shows the median longevity of the tracked whitings to be 5 days (mean = 5.02 days). **D)** Shows the median total current velocity from SLIM for these whitings locations to be 0.20 m/s^{-1} (mean = 0.16 m/s^{-1}). The minimum current velocity necessary to erode mud of the size fraction produced by whitings is 0.30 m/s^{-1} (gray bar), which must be exceeded to loft mud from the seabed into the water column, see text for details. In both box plots, notches-limits represent 5% confidence intervals around the medians, and whiskers span maximum and minimum values.

assuming unequal variance between datasets. Results are reported as *p* values, with values less than 0.05 considered significant.

Determining Whitings Longevity

To generate data on the persistence of whitings, we examined the 2012, 2014, and 2016 MODIS timeseries seeking periods where whitings behavior could be tracked across at least ten consecutive cloud-free days. Satisfying this criterion, February 1st through 11th, 2014, delivered 11 successive days of clear skies and 166 whitings counts. The satellite imagery showed the sea state to be calm throughout this timespan. For this 11-day period, individual whitings were tracked from one day to the next using three common-sense criteria to safeguard that a whiting present in the image acquired on February 2nd, for example, persisted for the 24 hours between MODIS overpasses, to be identified again on February 3rd, and so on.

The first criterion was that for a whiting to be considered persistent from one day to the next, it must not have drifted more than 1 km in the 24-hour period between MODIS observations. The second criterion for a persistent whiting is that if it has drifted, it has done so with a distance and direction compatible with the movement of its neighboring whitings. The idea here is that all whitings are drifting according to local prevailing currents and therefore should move in unison. If a whiting has moved in the opposite direction to its close neighbors, it is unlikely that a single whiting is being observed on consecutive days. Instead, a better explanation is that a new whiting has appeared in the population. The third criterion is that persistent whitings do not radically change in size from one day to the next.

Application of these criteria allowed the movement of 166 whitings to be followed for 11 days, from which statistics on longevity could be computed (Fig. 2). In addition, this whitings population could be framed in the context of the currents active on the platform top as simulated by the SLIM hydrodynamic model, as will be described in the following section.

SLIM Hydrodynamic Modeling

We simulated the currents around the Bahama Banks and atop them using the multi-scale ocean model SLIM (http://www.slim-ocean.be, accessed 12-12-2022). Unlike more traditional models, SLIM uses unstructured meshes, which are more flexible, to represent bathymetrically complex areas such as the shallow-water GBB. SLIM includes a 2-D module for shallow barotropic flows with wetting and drying, a 3-D module for density-dependent baroclinic flows, plus several different tracer transport modules (Hanert et al. 2003, 2005). This model has previously been used for a range of different applications such as estimating ecological connectivity in the Great Barrier Reef (Thomas et al. 2014; Grech et al. 2018; Figueiredo et al. 2022), modeling the freshwater plumes of the Congo and Columbia rivers (Le Bars et al. 2016; Vallaeys et al. 2018), transport of microplastics in the Bohai Sea (Li et al. 2018), and, most relevant, the hydrodynamics of GBB (Lopez-Gamundi et al. 2022). Here, we have used the 2-D version of SLIM with a mesh resolution of ~ 500 m over the entire Great Bahama and Cay Sal banks and a coarser resolution of approximately 10 km in the deep ocean. The platform-top bathymetry used in SLIM were taken from Purkis et al. (2014) for the Cay Sal Bank and Harris et al. (2015) and Purkis and Harris (2016) for GBB. The bathymetric models for both platforms were generated from extensive

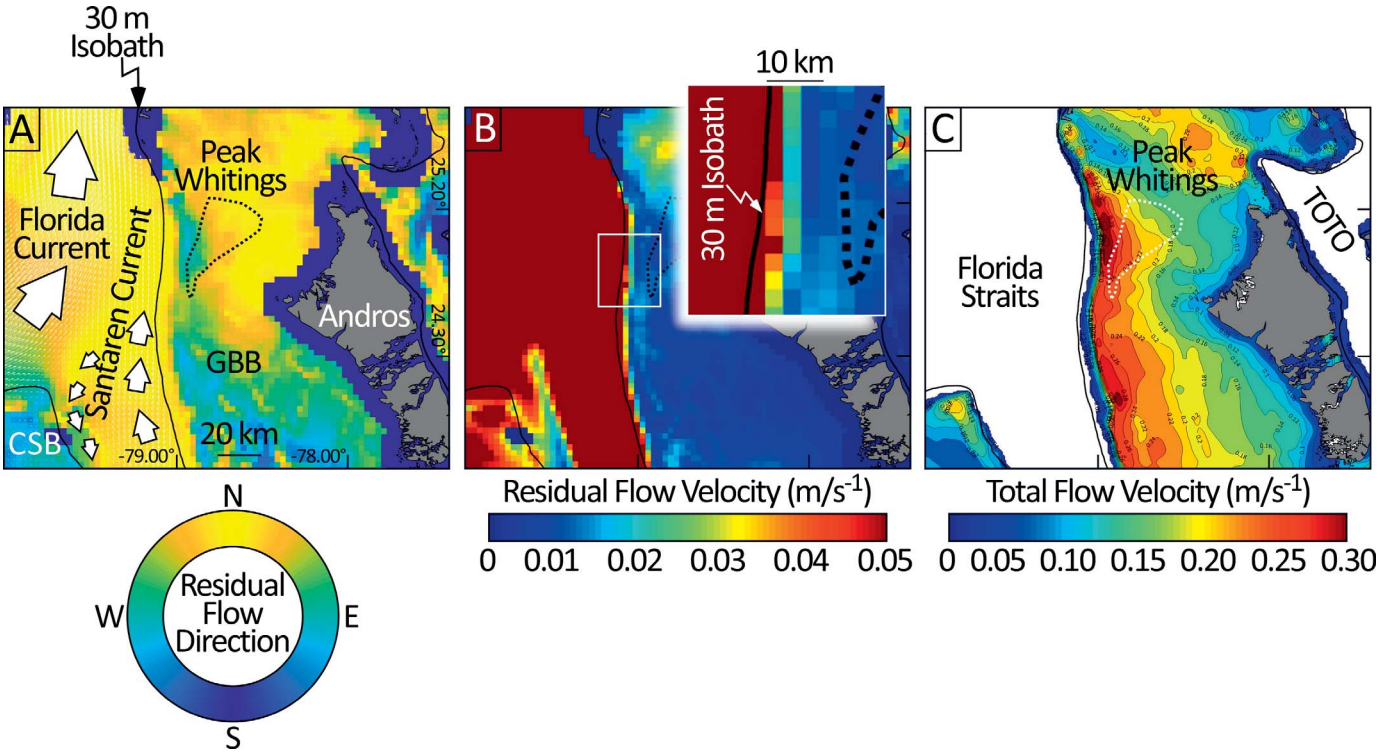

FIG. 3.—Averaged outputs from the SLIM hydrodynamic model for the period Jan. 1st through Feb. 28th, 2016, for the western Great Bahama Bank (GBB) and adjacent Florida Straits. The Cay Sal Bank (CSB) is situated in the bottom left of each frame, and the 30 m isobath (labeled) is taken to delineate the platform margins of both GBB and CSB. **A)** SLIM direction of residual flow, defined as flow prior to the addition of the tidal signal. **B)** Shows residual flow velocity. Note entrainment of platform-top waters in the Santaren Current up to 10 km inboard of the 30 m isobath, delivering a low-velocity (0.05 m/s^{-1}) northward residual flow (inset B). **C)** Contour map of total flow velocity (i.e., residual flow + tidal signal). Note accelerated flow of up 0.30 m/s^{-1} along the western GBB platform margin and to the north of Andros Island. SLIM predicts the former locality to be a site of enhanced exchange of platform-top and normal-marine waters from the Florida Straits, and the latter to exchange platform-top and normal-marine waters from the Tongue of the Ocean (TOTO). The zone of peak whitings, defined by Purkis et al. (2017), is situated between these two foci. See Supplemental Material for the full complement of 2016 bimonthly SLIM outputs.

single-beam sonar soundings, digitized nautical charts, and bathymetry derivation from high-resolution visible-spectrum satellite data using the workflow described by Purkis et al. (2019a). Note that although Little Bahama Bank lies within the model domain (full domain depicted in Fig. 1A), the SLIM-simulated currents atop this platform were not considered reliable because we have yet to generate a robust bathymetric model for this site. The simulation extends over two full years, from Jan. 2014 to Dec. 2014, and from Jan. 2016 to Dec. 2016, with a time step of 15 min. The main forcings are the wind from NOAA's Climate Forecast System Version 2 (CFSv2) Operational Analysis dataset, tides from OSU TOPEX/Poseidon Global Inverse Solution TPXO dataset (Egbert and Erofeeva 2002), with large-scale ocean circulation provided by the HYCOM + NCODA Global 1/12° Analysis (GLBu0.08) dataset (Fox et al. 2002; Cummings 2005; Cummings and Smedstad 2013). All these forcings were applied using a spin-up period of one day. SLIM was used to simulate multiple aspects of the on- and off-platform currents and the interaction between the two, including the direction and velocity of residual flow (Fig. 3A and B, respectively), and total flow (Fig. 3C). Residual flow is defined as that before the addition of the tidal signal, whereas total flow is the residual + the tidal signal. These outputs were used to model the water-age dynamics over the GBB and hence infer the spatial and temporal variability of water exchanges between the platform top and the deep ocean. For the sake of brevity, only results averaged over January and February 2016 are shown because the annual and seasonal variance of the SLIM outputs is minor. The full complement of bimonthly SLIM outputs (residual flow direction and velocity, and total flow) is provided as Supplemental Material.

Field Validation of the SLIM Model

SLIM outputs were verified in three ways of which two—validation with respect to HYCOM velocity outputs in the deep ocean, and with respect to tide-gauge measurements—were conducted continuously throughout the year-long model run. In the Florida Straits, SLIM currents are very close to HYCOM's depth-averaged currents, suggesting that the large-scale circulation is well reproduced. Lack of field observations prevented us from validating the model on GBB. The model has, however, been successfully validated against tide-gauge measurements on Little Bahama Bank (LBB) and in the Florida Reef Tract (Frys et al. 2020). The third verification of SLIM was facilitated by the passage of Hurricane Matthew over GBB in October 2016. This Category 4 storm served to suspend vast quantities of sediment atop GBB and, given the clear skies in the days following Matthew, the dissipation of this plume by platform-top currents could be observed by daily satellite passes (Fig. 4A) and compared to the SLIM flow predictions from 2016 (Fig. 4B). Though this comparison is qualitative, reassuringly, the plume was preferentially dispersed from the same areas predicted by SLIM to have accelerated flow.

A Platform-Top Model of Aragonite Saturation State

To test our hypothesis that hydrodynamic mixing of on-platform and off-platform water masses of different temperatures influence the localization and frequency of whitings, we first audited satellite-derived sea-surface temperatures for our region of interest from the GHRSST L4 Global Foundation SST (Chao et al. 2009). Bimonthly-averaged GHRSST

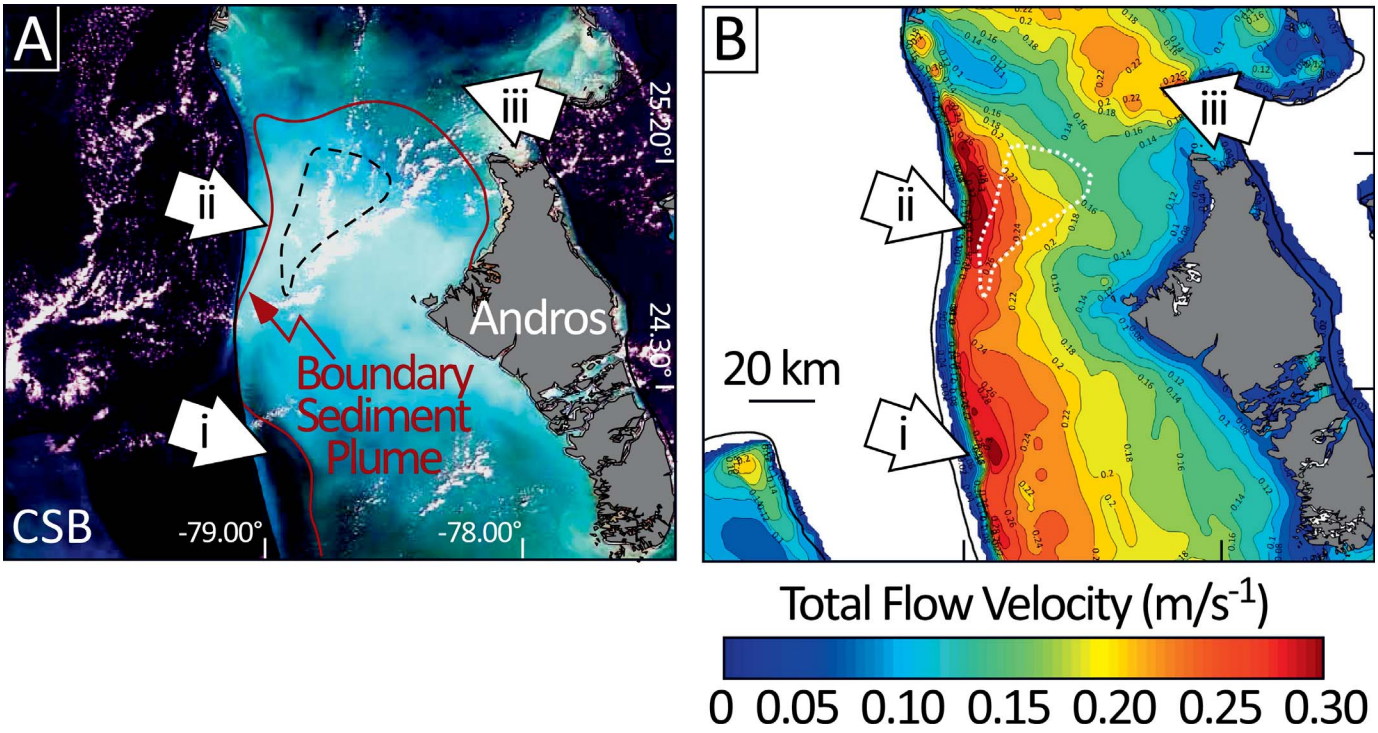

FIG. 4.—Qualitative validation of the SLIM model from dispersion of a storm-lofted sediment plume. **A)** MODIS Aqua satellite image from Oct. 8th, 2016, two days after the passage of Category 4 Hurricane Matthew, showing a vast sediment plume (boundary delineated with maroon line) extending from the west coast of Andros Island to the western margin of Great Bahama Bank. Arrows (i–iii) show how the plume has been preferentially dispersed at the three localities where the SLIM model predicts **B)** accelerated platform-top flow.

data from 2016 were used to set temperatures of both water masses in the model as audited inside two 225 sq. km areas, one atop the GBB and one situated off-platform in the normal marine waters of the adjacent Florida Straits (Fig. 5A, Table 1). The GHRSST L4 data have a 1 km spatial resolution and, being derived from satellites operating in both the infrared and microwave spectrums, are free from cloud contamination.

Carbonate chemistry of the waters atop Great Bahama Bank is known to vary through both space and time (Broecker and Takahashi 1966; Morse et al. 1984, 2003; Robbins et al. 1997; Broecker et al. 2000; Geyman and Maloof 2019; Geyman et al. 2022), and thus we conducted a second model iteration that incorporates spatial heterogeneity in seawater chemistry to evaluate the impacts of mixing on water masses characterized by both thermal and compositional differences. Inconveniently, no published data exist describing the carbonate chemistry of the Bahamas with spatial fidelity applicable to this study. The only relevant data are at regional scale (Rosón et al. 2003; Schuster et al. 2013; Woosley et al. 2016; Wanninkhof et al. 2019). Most pertinent to our study is Wanninkhof et al. (2019), who integrated > 1 million *in situ* measurements of SST, sea-surface salinity (SSS), and fugacity of carbon dioxide in surface waters (fCO_{2w}) with remotely sensed SST and SSS and empirical correlations with the carbonate system (Gledhill et al. 2008). The product of this analysis is a Caribbean-wide grid of SSS, total alkalinity, and pH with a resolution of 1° × 1°. Using these data from Wanninkhof et al. (2019; available at www.aoml.noaa.gov/ocd/gcc, accessed 01-12-2022), we extracted monthly SSS and pH values for 2016 from the two grid cells representing on-platform (25.5° N, –78.5° W) and off-platform (24.5° N, –79.5° W) water masses. Sea-surface temperatures for each water mass within each time period (Table 1) were extracted from the GHRSST cube as described above. Any unit conversions in ionic concentration were conducted using Geochemist's Workbench v. 12.0 (Bethke and Yeakel 2018), hereafter "GWB" for brevity. For example, Drever (1988) reports HCO_3^- concentrations, which were converted to CO_3^{2-} concentrations in mg/kg by assuming elemental equivalents calculated within GWB. For each bimonthly pair, available values of observed sea-surface salinity ("SSS_OBS") and pH (calculated in CO_2SYS using equations in Cai et al. 2010, listed as "average_pH[Cai]" in Wanninkhof et al. 2019) were averaged for observations collected in both on-platform and off-platform water masses (Supplemental Table 1). In this calculation, pH from the gridded dataset was used directly in GWB. Using normal marine chemistry from Drever (1988, Supplementary Table 2), we assumed conservative behavior of all ions relative to salinity, and calculated salinity-normalized values for Ca^{2+}, Mg^{2+}, Na^+, K^+, CO_3^{2-}, SO_4^{2-}, and Cl^- (Supplemental Tables 3, 4) that reflect the changes in *in situ* salinity values presented by Wanninkhof et al. (2019). Note that our conceptual model is simplified compared to natural conditions because we assume conservative behavior of all elements out of necessity: platform-top chemistry data with sufficient density and temporal resolution are unavailable, and not all ions are likely to behave conservatively through both space and time (i.e., Broecker and Takahaski 1966; Geyman and Maloof 2019; Geyman et al. 2022) which can impact W_{arag}. In addition, although biological processes such as photosynthesis and respiration are likely relevant to whitings formed via water-column precipitation (Robbins et al. 1997), these reactions are not included in our simulation. Further work constraining biological activity, as well as variability in seasonal ranges of the carbonate system and trace-element concentrations at the resolution of our hydrodynamic model, is warranted, but our initial model provides fundamental insight into the relationship between hydrodynamic mixing and Ω_{arag} atop GBB.

To calculate the degree of aragonite saturation, we employed numerical models in GWB using the built-in thermodynamic database thermo_phreeqc, which was compiled from the phreeqc.dat release 2.8 by Daniel Saalfeld and Craig Bethke (https://www.gwb.com/thermo.php, accessed 15-08-2022). All speciation calculations conducted here employ the

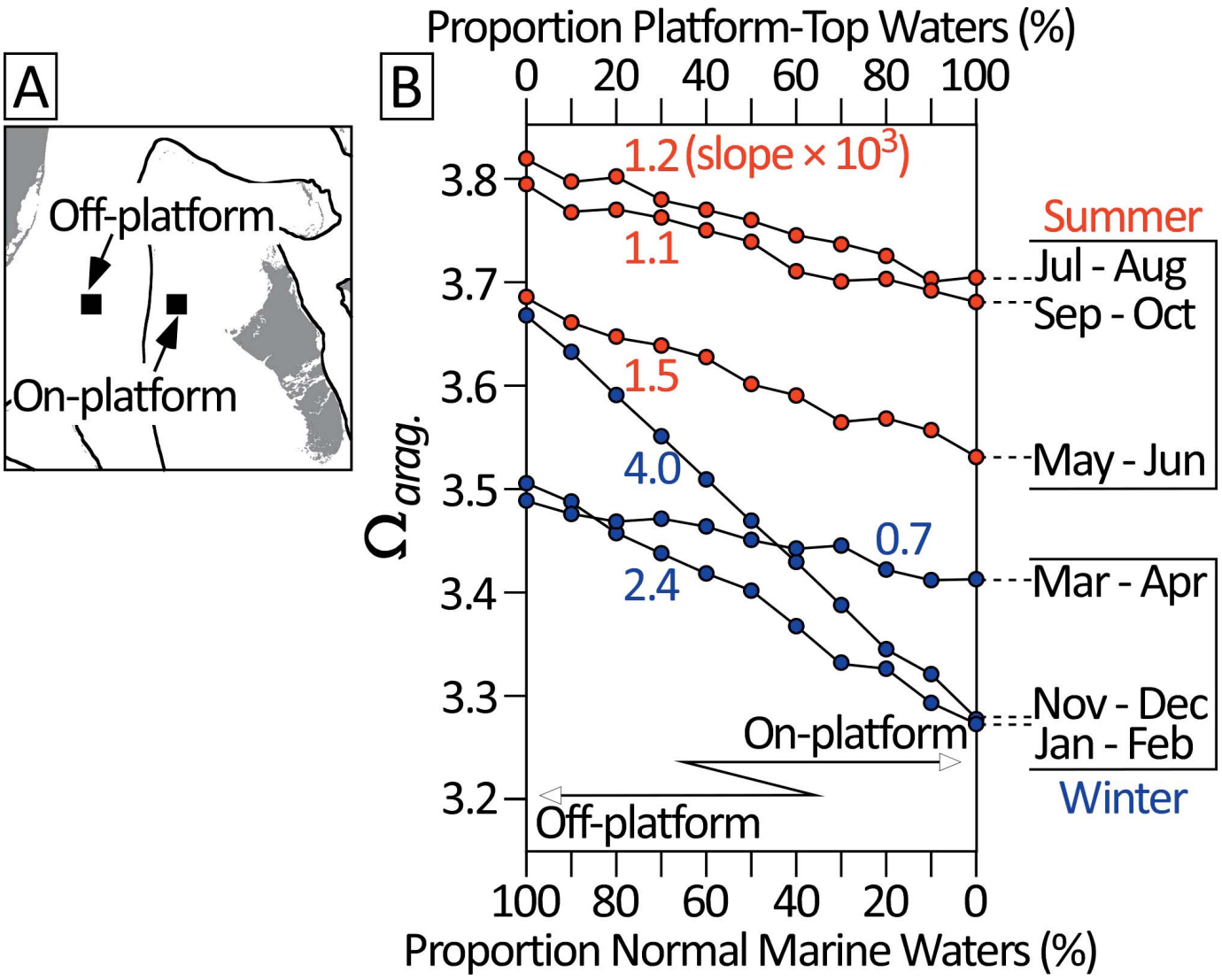

FIG. 5.—**A)** Bimonthly averages of sea-surface temperature audited within two 225 sq. km areas for 2016. The first area is located atop GBB platform in the lee of Andros Island (and in the zone of peak whitings production), and the second is located 50 km off the western platform margin in the normal marine waters of the Florida Straits. These temperature records were used in the calculation of mixing of off-platform and on-platform water masses in Geochemist's Workbench to calculate the degree of bimonthly aragonite saturation (Ω_{arag}) **B)**. The right side of the *x* axis represents the situation of the most restricted waters (i.e., 100% platform-top waters, 0% normal marine), and the left side is the reciprocal configuration (0% platform-top waters, 100% normal marine). With the exception of Mar–Apr, note that the slope ($\times 10^3$) of Ω_{arag} for the three summer bimonthly mixtures (i.e., May–Jun, Jul–Aug, and Sep–Oct) are lower than the equivalent winter months. This trend suggests that winter mixing of on- and off-platform waters will have a larger impact on Ω_{arag} because the temperature differential between the two water bodies is greater.

Debye-Hückel equations (translated by Robinson and Stokes 1968) for activity coefficients as originally calculated in the PhreeqC thermodynamic database above. Model results are reported as the degree of saturation of aragonite (W_{arag}) according to:

TABLE 1.—*Minimum, maximum, and sea-surface temperature (SST) differentials used in Geochemist's Workbench to model the degree of aragonite saturation for each bimonthly pair.*

T°C	Jan–Feb	Mar–Apr	May–June	July–Aug	Sept–Oct	Nov–Dec
Minimum SST (*On Platform*)	21.84	24.71	27.49	29.77	28.68	24.36
Maximum SST (*Off Platform*)	26.42	26.27	28.91	30.96	29.80	27.71
Maximum ΔSST	4.58	1.57	1.42	1.18	1.12	3.36

$$\Omega = \frac{Q}{Ksp} \quad (1)$$

where Q is the ion activity product and K_{sp} is the solubility product at equilibrium for aragonite.

A series of ten calculations mixing off- and on-platform water masses were conducted in the Geochemist's Spreadsheet module of GWB for each bimonthly pair using the "smart mix" function in 10% increments (i.e., 90% off-platform, 10% on-platform) which was interpolated to 1% increments via regression, with resulting seawater-composition charge balance constrained by chloride concentrations.

Mapping the Spatial Variability in the Degree of Aragonite Saturation

To integrate our diverse datasets, including hydrodynamic environments derived from the SLIM model (Fig. 3), Ω_{arag} modeled in Geochemist's

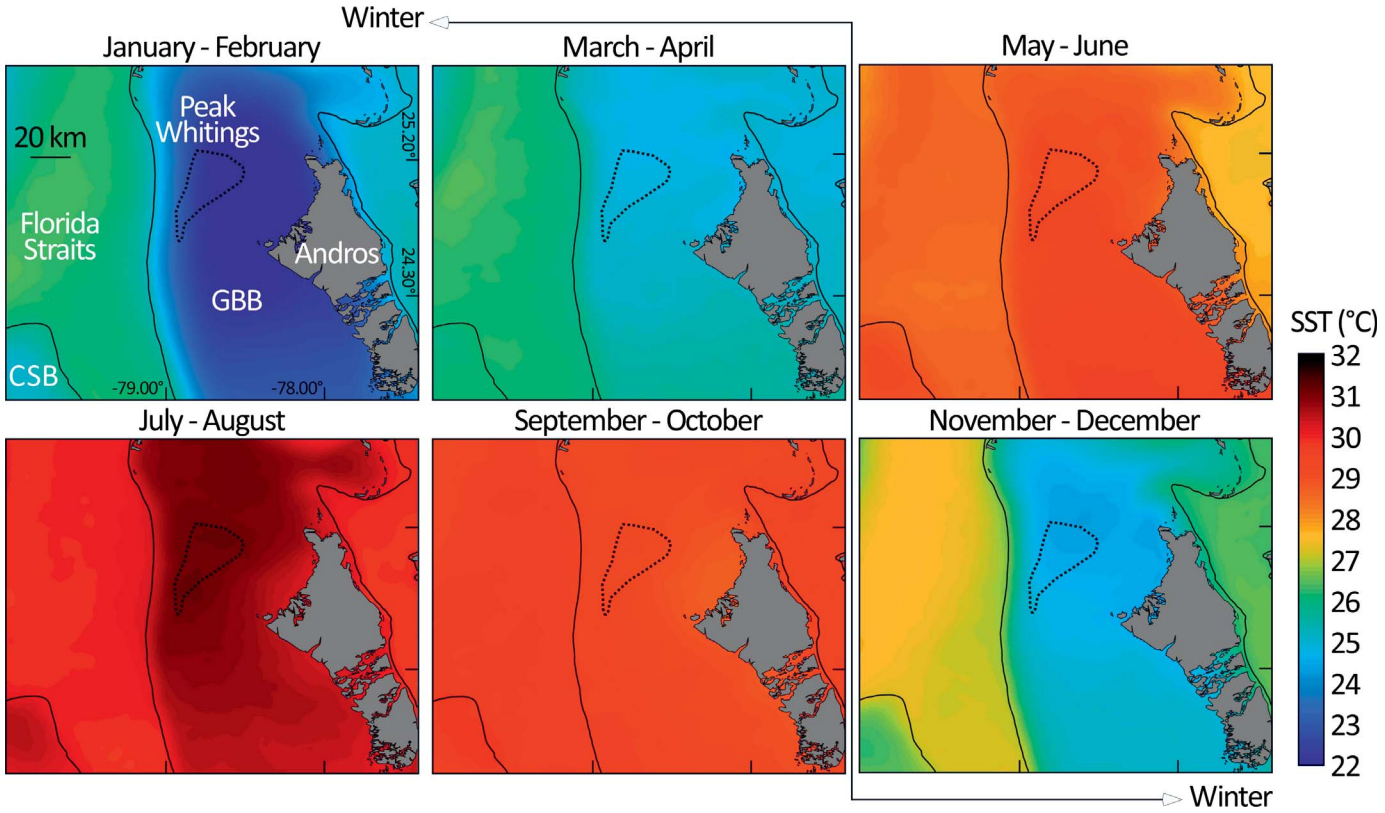

FIG. 6.—Bimonthly averaged sea-surface temperature (SST) through 2016 extracted from the GHRSST L4 Global Foundation dataset (Chao et al. 2009) for the western Great Bahama Bank (GBB) and adjacent Florida Straits. The Cay Sal Bank (CSB) is situated in the bottom left of each frame. In the six winter months (Nov–Apr), pronounced temperature differentials of up to 5 °C locally exist between the cold GBB platform-top waters and the warmer Florida Straits. This differential is absent in the six summer months (May–Oct).

Workbench (Fig. 5 and Supplemental Table 3), and sea-surface temperature (SST) audited via remote sensing (Chao et al. 2009) (Fig. 6), a mesh was generated across the platform top with nodes spaced at 0.01°. An example of the spatial inputs from January 15th, 2016, and the 0.01° grid created for interpolation is shown in Figure 7. The minimized distance of every platform-top node to the platform margin was computed and then the mean annual SLIM flow velocity was convolved to produce a surface which tends towards 100% normal marine water when the node is near to the margin and the predicted SLIM flow rate is high. Such areas are considered to be well flushed, have a low residence time, and have chemistry akin to normal-marine waters. In contrast, nodes situated in the platform interior and with low rates of SLIM flow, logically representing more restricted conditions, tend towards 0% off-platform water in the computed surface (Fig. 7B). The Ω_{arag} that reflects the proportion of normal marine seawater could then be assigned for each node on the mesh for each bimonthly pair with reference to the previously calculated look-up table computed in GWB (Supplemental Table 3). The resultant mixing proportions for on- and off-platform waters was interpolated onto continuous surfaces. Resultant daily maps were averaged into bimonthly pairs (Fig. 8) from which bimonthly Ω_{arag} statistics could be extracted for the 2,270 whitings digitized from 2016 MODIS imagery (Fig. 9).

RESULTS

Frequency and Area of Whitings

Frequency of whitings in 2016 data mapped in this study are consistent with that presented by Purkis et al. (2017); namely, whitings are significantly more frequent in winter months than in their summer counterparts ($p < 0.05$) (Fig. 10A). Subdividing GBB into precincts north and south of Williams Island, a convenient landmark situated in the center of the latitudinal range of whitings occurrence (see Fig. 1B), allow a comparison of both the frequency of the 2016 whitings and their area (note that our whitings counts for 2012 and 2014 lack data on their areal extent and therefore cannot be considered in this way). On average, whitings from 2016 that occurred in the precinct of GBB north of Williams Island (Fig. 10, yellow region) are both more frequent (Fig. 10A, Table 2, $p < 0.05$) and larger (Fig. 10B, Table 2, $p < 0.05$) than those forming in the southern precinct (Fig. 10, blue region). This behavior in the spatial distribution of 2016 whitings is consistent with the zone of "peak whitings" as defined by Purkis et al. (2017) (see Fig. 1B, this paper) which is situated in the precinct north of Williams Island. As presented in Figure 4B of Purkis et al. (2017), summer whitings (May through Oct.) occur most frequently in, or in close proximity to, the peak whitings zone. Winter whitings (i.e., those occurring in Nov. through Apr.) have a wider spatial distribution and appear as far south as the tidal outflows—locally called "bights"—that separate Big Wood and Mangrove cays in the southern half of Andros Island. This seasonal difference in whitings occurrence is also evident in the 2016 whitings digitized for this study (Fig. 8).

The Longevity of Whitings

February 1st–11th, 2014, provides a span of cloud-free days where the behavior of 166 whitings can be tracked across 11 consecutive MODIS overpasses (Fig. 2). Tracking this population reveals the median longevity of the whitings to be 5 days (mean = 5.02 days). Extracting the total current velocity from the SLIM model for the same time periods predicts the

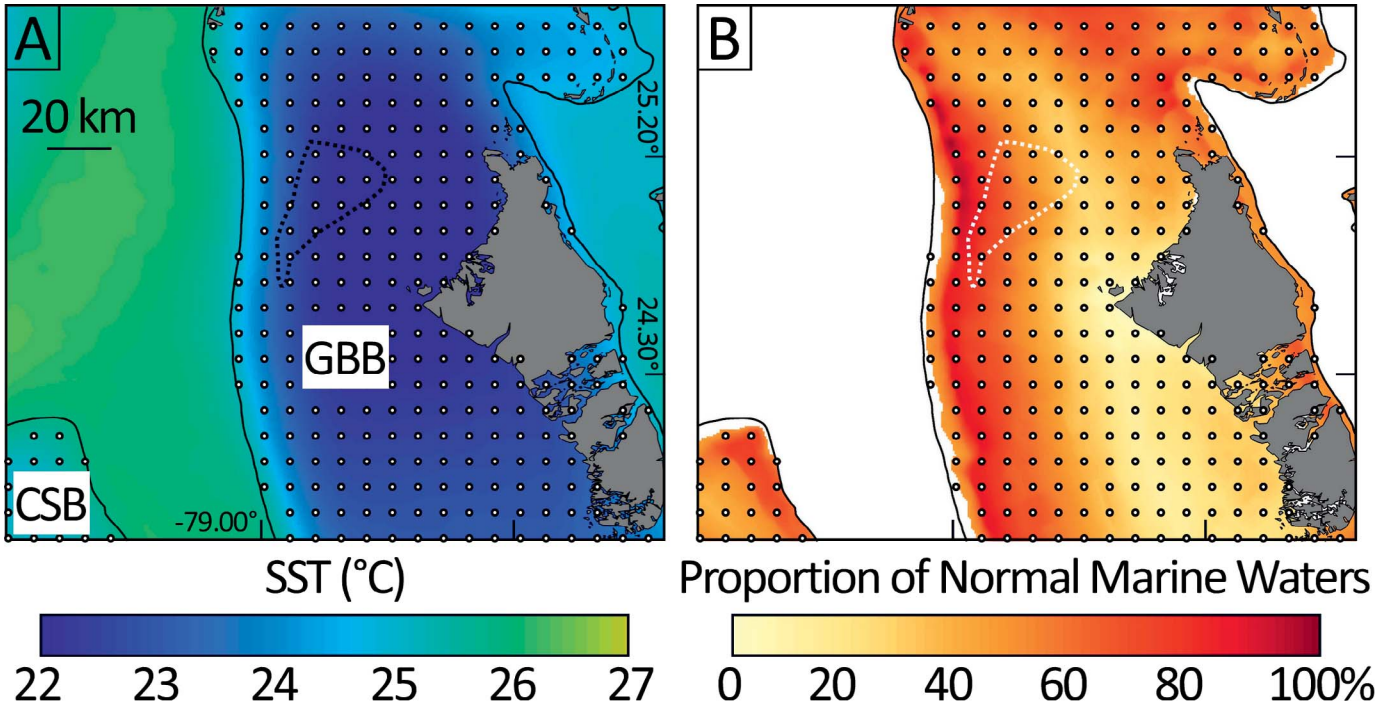

FIG. 7.—Spatial inputs for the computation of daily platform-top aragonite saturate state (Ω_{arag}). Dots represent nodes of the 0.01° grid at which daily **A)** GHRSST L4 sea surface temperature and mixing of on- and off-platform waters as predicted by **B)** SLIM were audited. Data taken from Jan. 15th, 2016. Zone of peak whitings delineated as broken black and broken white polygons in Parts A and B, respectively.

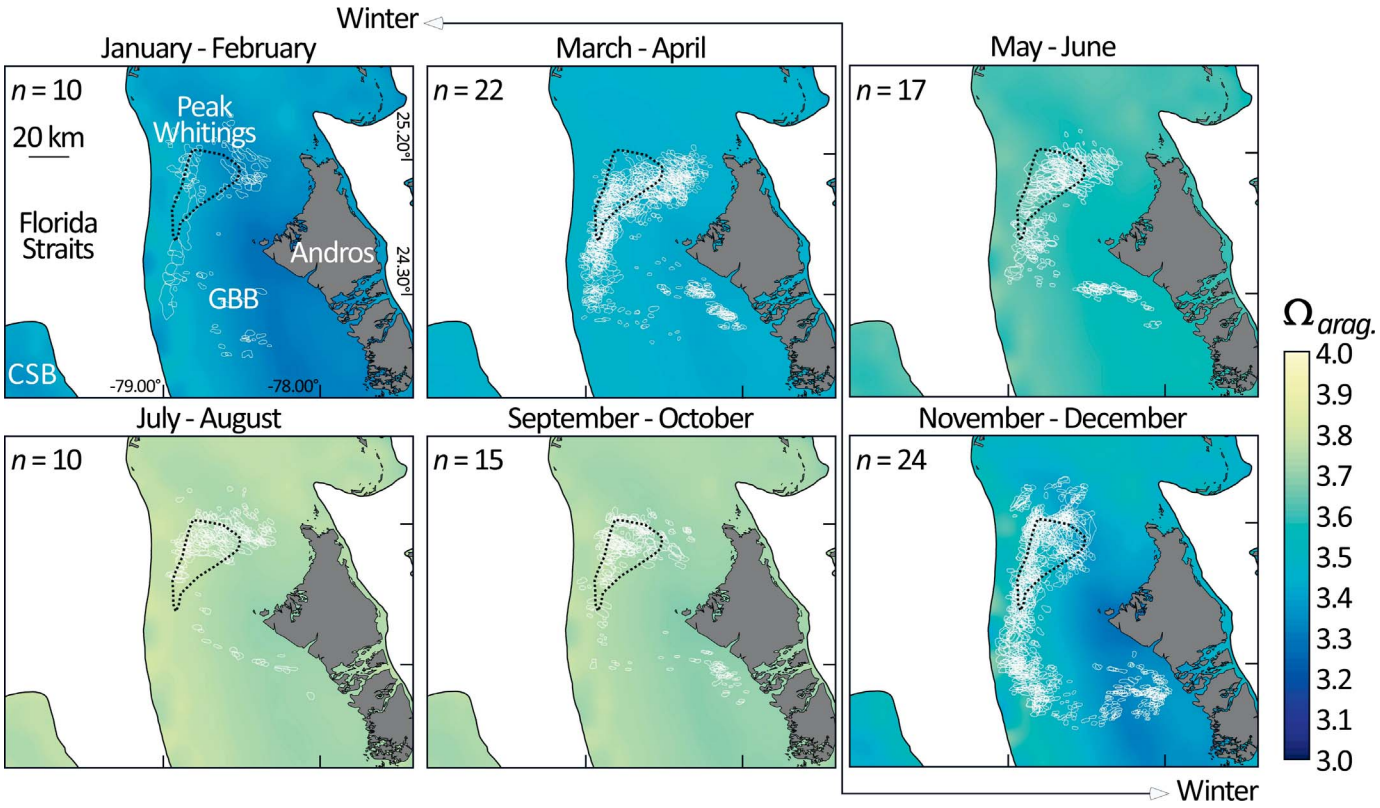

FIG. 8.—Bimonthly maps of platform-top aragonite saturation state (Ω_{arag}) for the Great Bahama and Cay Sal banks (GBB and CSB, respectively) computed with reference to sea-surface temperature and the mixing of on- and off-platform waters. See text for details. Note that Ω_{arag} is higher in summer than winter, matching thermodynamic expectations, but the winter months exhibit higher spatial variability. White polygons in each map demark the boundaries of the 2,270 whitings digitized from 2016 MODIS imagery. The *n* in the top-left of each pane specifies the number of cloud-free days mapped in each bimonthly pair.

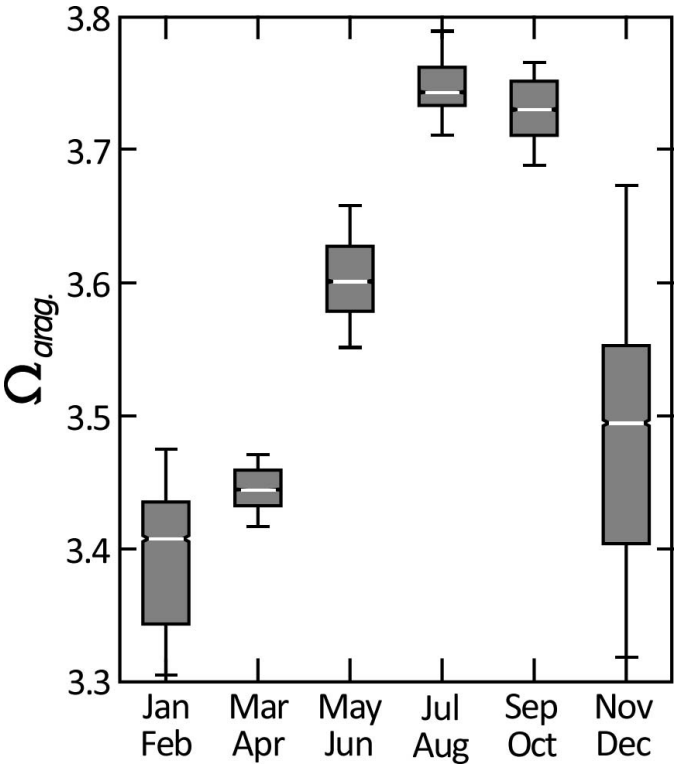

FIG. 9.—Boxplot of bimonthly aragonite saturate state (Ω_{arag}) for the 2,270 whitings digitized from 2016 MODIS imagery. For each box, horizontal white line is median Ω_{arag}, top and bottom of box are 75th and 25th percentiles, respectively, and whiskers represent maximum and minimum values. Ω_{arag} is highest in summer, but the winter months exhibit greater variability.

median current velocity at the whitings locations to be 0.20 m/s^{-1} (mean = 0.16 m/s^{-1}).

SLIM: A Multiscale Hydrodynamic Model

Despite nearly one-order-of-magnitude difference in fidelity, the SLIM results are comparable to those generated by Purkis et al. (2017) using the cruder-resolution MIKE-3 model. Namely, both identified enhanced rates of flow across the platform margin, driven predominantly by tidal currents, with flow decreasing with distance inboard from the margin. These results are in accordance with the distribution of platform-top facies; high-energy oolitic grainstone shoals locally rim the margin and fine-grained deposits are observed farther inboard (Enos 1974; Kaczmarek et al. 2010; Reijmer et al. 2009; Harris et al. 2015; Purkis and Harris 2016; Wu et al. 2021). SLIM represents two important advances over MIKE 3, the first being that it is better validated by tidal measurements within the model domain. The second advantage is that SLIM is solved on a grid which is one order finer than that of MIKE 3. It therefore offers superior insight into patterns of flow atop GBB. Although situated up to 50 km inboard of the western platform margin, the SLIM model predicts the zone of peak whitings to be positioned in an area which is regularly nourished by normal marine waters. The flushing of the peak whitings zone by normal marine waters in this zone comes from two opposing directions (Fig. 3C). First, across the western platform margin where normal marine waters are introduced from the Florida Straits and second, from the northeast, with normal marine waters flowing from Tongue of the Ocean around the northern tip of Andros Island. The SLIM model predicts that these flows are driven primarily by tidal currents, not resultant of residual flow as set up by winds and off-platform currents (Fig. 3B vs. C). This said, residual flow does drive at least some exchange of normal-marine with platform-top waters. As emphasized in Figure 3A, SLIM predicts that the northward-flowing Santaren Current entrains platform-top waters up to 10 km inboard of the margin, delivering northward residual flow, albeit of limited velocity (< 0.05 m/s^{-1}). Mixing of normal-marine and platform-top waters, whether by residual or tidal currents, has important implications for the carbonate chemistry of the GBB, described in the following section.

Mapping Spatial Heterogeneity of Ω_{arag}

Results of mapping Ω_{arag} across GBB for bimonthly pairs in 2016 (Fig. 8) show that the highest Ω_{arag} is observed in summer (Jul–Aug, $\Omega_{arag} = \sim 3.8$), while the lowest overall Ω_{arag} is observed in the winter (Jan–Feb, $\Omega_{arag} = \sim 3.3$). Winter months exhibit the highest spatial heterogeneity in Ω_{arag} (Fig. 8) and the highest variability in Ω_{arag} (Fig. 9), and deliver the most frequent and largest whitings (Fig. 10). In contrast, the summer months exhibit the opposite trends in all these parameters. Spatial heterogeneity in winter Ω_{arag} is interpreted to be driven by the stark temperature disparity between on- and off-platform waters that exists between November and April (Fig. 6), and the mixing off these disparate water bodies by prevailing platform-top circulation (Supplemental Figs. 1–3). Higher Ω_{arag} values are observed near the western margin of GBB and to the north of Andros Island during the winter months (Fig. 8).

DISCUSSION

Longevity Suggests that Whitings are Not Resuspended, but Replenished by Direct Precipitation

Tracking 166 whitings across 11 cloud-free MODIS overpasses (Fig. 2A, B) shows individual whitings in this population to have a median (and mean) persistence in the water column of five days (Fig. 2C). SLIM modeling predicts the tracked whitings to inhabit a hydrodynamic flow regime during this 11-day period with a median total current velocity of 0.20 m/s^{-1} and mean total velocity of 0.16 m/s^{-1} (Fig. 2D). This observation and the model output are relevant to whether whitings consist of mud resuspended from the seabed, or whether they originate from the direct precipitation of aragonite in the water column. Two parameters are important here, of which the first is the current velocity that must be exceeded to erode and loft mud from the seabed. Second, once in suspension, important is the time required for the mud to settle out of the water column.

To the first of these parameters, erosion velocity as a function of grain size has been studied for nearly a century. Both Shinn et al. (1989) and Robbins and Blackwelder (1992) collected seawater from active whitings atop GBB, filtered the aragonitic mud in suspension in those waters, and ascertained that the nonaggregated aragonite crystals that constitute whitings vary between 2- to 4-μm in diameter. According to the foundational work of Hjulström (1935), a current velocity of at least 0.30 m/s^{-1} would be required to erode and suspend this size fraction from the seabed. This velocity should be considered conservative because the mud blanket that underlies the whitings zone on GBB is heavily bound by cyanobacterial biofilms (and their mucilaginous secretions), which increases the erodibility velocity by a factor of at least three, but up to a factor of nine in cases of particularly dense microbial colonization (Neumann et al. 1970). By contrast, our SLIM model advocates that the whitings that we could track from MODIS experienced mean currents moving at 0.16 m/s^{-1}, only half the erodibility velocity of whitings mud on even an uncolonized seafloor. Our results are thus in harmony with the field observations of Shinn et al. (1989), who report that current speeds in the vicinity of active whitings are insufficient to erode bottom sediments. The authors also noted that the currents measured in whitings were not detectably different from those measured in the clear waters surrounding whitings, suggesting that localized acceleration of flow which might occur

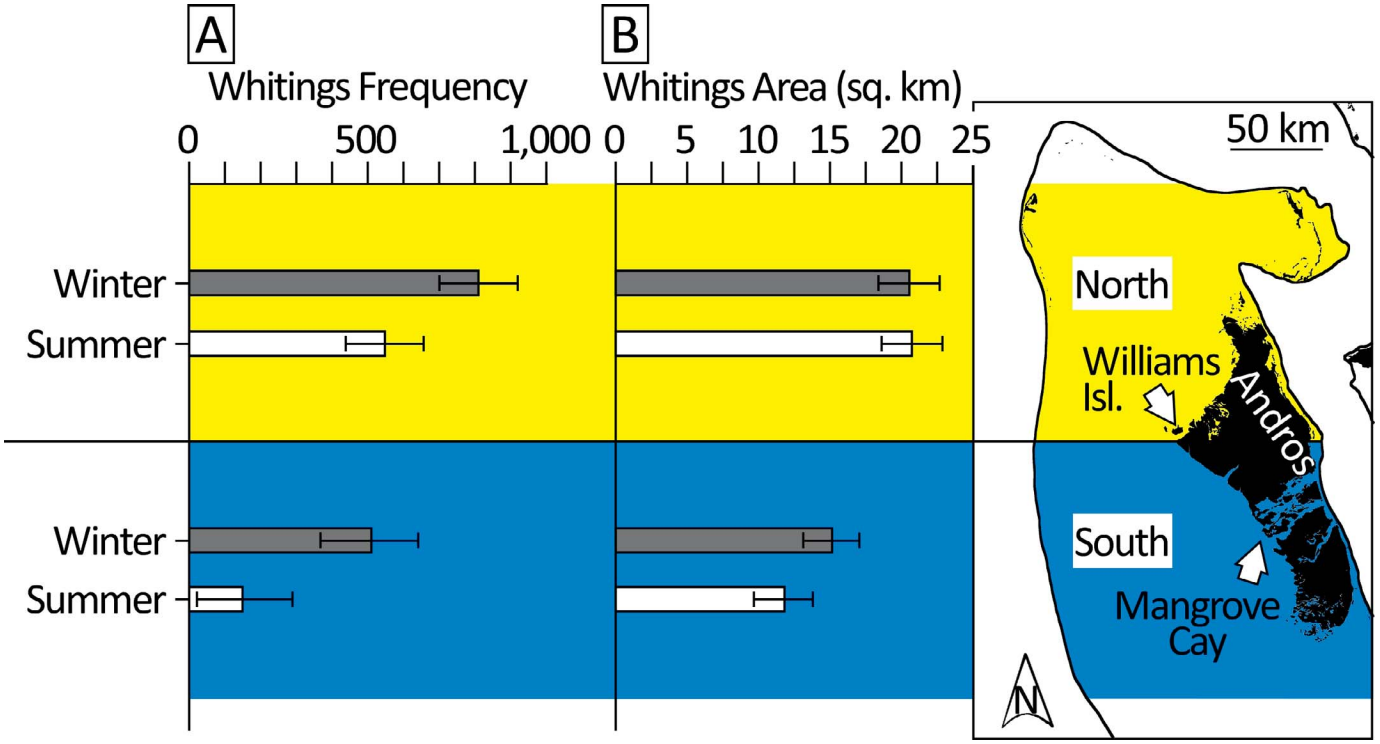

FIG. 10.—**A)** Frequency and **B)** area of 2016 whitings separated into precincts north (yellow) and south (blue) of Williams Island, a convenient landmark situated just off the west coast of Andros Island on Great Bahama Bank (GBB). Whitings in the northern precinct are similarly sized ($p = 0.7744$) and occur at similar frequency ($p = 0.535$) seasonally, while whitings in the southern precinct are larger ($p = 0.0082$) and more frequent ($p = 0.0000$) in the winter. In the winter months (Nov–Apr), northern precinct whitings are larger ($p = 0.0002$) and more frequent ($p = 0.0173$) than those in the southern precinct, a trend that is consistent in summer months (May–Oct) as well ($p = 0.0000$, and $p = 0.000$, respectively, Table 2). Error bars represent standard error.

at a scale finer than the 500 m resolution of the SLIM model is not a factor in this phenomenon, as might be induced, for instance, by Langmuir circulation (Dierrssen et al. 2009). Further, if currents in the whiting zone routinely exceed the erodibility velocity for mud, even locally, it would be expected that the > 17,000 sq. km mud drape situated to the west of Andros Island would be winnowed away, which is clearly not the case (Reijmer et al. 2009; Purkis and Harris 2016). Though beyond the scope of this study, note too that whitings also abundantly occur in the Bight of Abaco on the Little Bahama Bank (Lloyd 2012; Larson and Mylroie 2014; Yao et al. 2023), a shallow 3,500 sq. km basin enclosed on three sides by islands. By virtue of the shelter afforded by these islands, it might reasonably be assumed that the currents in this bight are considerably less vigorous than those in the whitings zone of GBB, which is sheltered only on its eastern side (by Andros Island).

Neither does the persistence of the whitings that we tracked atop GBB support their genesis to be from resuspended bottom sediment. Field measurements made by Shinn et al. (1989) constrain the average particulate concentration in a whiting to be 0.01 g/L (equating to 10 g of material per 1 m^2 of a whiting). Averaging over 24 separate measurements, the same authors report that the suspended load settled at an average rate of 13.40 $g/m^2/hr$, concluding that this rate of sedimentation would dissipate a whiting within a few hours if the material in suspension is not continually being replenished. Given that the average water depth in the whitings zone is 4 m, as mapped by Harris et al. (2015), the experiments conducted by Shinn et al. would indeed suggest that if not continually replenished by precipitation, a whiting would settle out of suspension well within the 24 hrs. that separate two successive overpasses by the MODIS satellite. Yet, our tracking of 166 whitings over 11 days shows that their average lifespan is ~ 120 hrs. (5 days). Tracking whitings from MODIS has limitations, and the average whitings five-day lifespan should be considered conservative because a proportion of the population of whitings imaged on Feb. 1st, the start of the run of cloud-free images, almost certainly appeared at some unknown time before that date. Similarly, the run of cloud-free images finishes on Feb. 11th and a proportion of the tracked whitings undoubtably persist past that date. Too, the area of whitings shortly after their formation and shortly before their final dissipation will be smaller than the 0.06 sq. km area of a MODIS pixel, and therefore undetectable.

Even ignoring this artificial truncation of our tracking approach, the five-day average whiting lifespan is already two orders of magnitude too long to be explained by the resuspension of seabed mud. Plus, our modeling shows that the currents active in the whitings zone are too weak to even loft mud, let alone keep it in suspension for meaningful amounts of time. Based on this evidence, we conclude that whitings result from the direct precipitation of carbonate in the water column, not resuspension, as has been supposed too by Smith (1940), Shinn et al. (1989), Robbins and Blackwelder (1992), Schultze-Lam et al. (1997), Robbins et al. (1997), Thompson et al. (1997), Yates and Robbins (1998), and Swart et al. (2014).

TABLE 2.—*Results of two-tailed Student's t-test assuming unequal variance, reported as p-values. Statistically significant p-values (< 0.05) are bold and starred.*

	Whitings Per Day	Whitings Area (sq. km)
Summer vs. Winter, Northern Precinct	0.0535	0.7744
Summer vs. Winter, Southern Precinct	**0.0000***	**0.0082***
Northern Precinct Winter vs. Southern Precinct Winter	**0.0173***	**0.0002***
Northern Precinct Winter vs. Southern Precinct Summer	**0.0000***	**0.0000***

An Interplay between Hydrodynamics and Seawater Chemistry Sets the Stage for Whitings

Data assembled in this study (Figs. 1, 10), by Purkis et al. (2017), and by Yao et al. (2023) affirm that whitings frequency atop GBB is significantly higher in winter than summer months. Peak frequencies are observed in early December and February (Fig. 1D) coincident with the largest spatial extent of whitings (Fig. 10). Despite inherent differences in data collection methods, previous studies of the seasonality of GBB whitings document similar temporal trends. In studies based on NASA astronaut photos spanning 1963–1993, for instance, Tao (1994) and Robbins et al. (1997) describe more frequent whitings near the margin of GBB, with peak whiting spatial extent occurring in April and again in October. More recently, Lloyd (2012) counted whitings on LBB and GBB from MODIS imagery spanning 2000–2010 and revealed higher frequencies and larger spatial extents of whitings observed in the winter months.

The phenomenon of amplified winter whitings is not restricted to the Bahamas. Also using MODIS, the same winter bias has been observed off Southwest Florida (Long et al. 2014; Long 2016) and in the Persian/Arabian Gulf (Shanableh et al. 2019). In the former case, manual counts spanning 2003–2018 document a higher proportion of winter whitings, but also a statistical relationship between nearshore whiting events and SST within 20 km of the coast (Long 2016). In the latter case, whitings in the Persian/Arabian Gulf occurred exclusively in the winter months, with a peak frequency in February—in line with our own GBB observations. These studies from Florida and the Gulf suggest that enhanced winter whitings are not a Bahamian quirk. Rather, they appear to be a general rule in the modern environment and provide new insight into the decades old controversy. We interpret the literature and our own results to signify that a hydrodynamic regime in which temperature-differentiated water masses are mixed can act to set the stage for hyper-localization of whitings formation. By extension, the same process imposes seasonality on the production of whitings mud. Further, the amplification of winter whitings through the mixing of warm and cold waters is agnostic as to whether they are ultimately triggered biogenically (e.g., Cloud 1962; Robbins and Blackwelder 1992; Swart et al. 2014; Lisle and Robbins 2016) or are purely abiotic precipitates (e.g., Black 1933; Bustos-Serrano et al. 2009; Morse et al. 1984, 2003). Either or both triggers would be boosted by the increase in Ω_{arag} that mixing induces. For this reason, in the rest of this discussion we will *evaluate the impact of spatial trends in sea surface temperature driven by hydrodynamic regime only* in generating localized zones of favorable conditions for the initiation of whitings produced through water-column precipitation, whether biologically influenced or otherwise.

Enhanced Winter Whitings are Contrary to Theoretical Expectations

Elevated frequency and size of winter whitings is counter to thermodynamic expectations of water-column precipitation for at least three reasons. First, as shown in the satellite observations of SST for GBB (Fig. 6), platform-top waters are substantially warmer in summer than winter. Given that CO_2 solubility decreases with increasing temperature, warm summer platform-top waters will tend to release CO_2 to the atmosphere, raising their pH, resulting in more favorable Ω_{arag} for carbonate precipitation. Second, and in the same vein, photosynthesis rate increases with increasing temperature, and the waters atop GBB are well stocked with photoautotrophs, including cyanobacteria and picoplankton (Smith 1940; Shinn et al. 1989; Robbins and Blackwelder 1992; Robbins et al. 1997; Thompson et al. 1997; Yates and Robbins 1998, 2001; Swart et al. 2014). Accordingly, enhanced summer photosynthesis further decreases the concentration of dissolved CO_2 in the warm platform-top waters, in theory, again, raising the likelihood of whitings precipitation. The third reason why a dominance of winter whitings is unexpected is that, withstanding hurricanes, summer GBB waters are more quiescent than winter, conditions which have been proposed to be more conducive to lime-mud precipitation (Granier 2012).

The fact that whitings seasonality defies theoretical expectations points to an alternative trigger which evidently overrides our assumptions of thermodynamics. Assembled data suggest that this trigger is related to the strong winter temperature disparities that exist between on- and off-platform waters, which can be as high as 5 °C in bimonthly-averaged SST (e.g., Nov–Dec, Fig. 6). Recent modeling efforts suggest that warming Bahamian waters by $\sim$ 12 °C can increase the carbonate precipitation flux by a factor of 5.5×, highlighting the importance of temperature differentials in the carbonate system (Geyman et al. 2022). These stark temperature differentials develop when the shallow bank-top waters equilibrate more rapidly with the atmosphere during the passage of winter cold fronts, relative to the more deeply mixed off-platform waters, as proposed by Ginsburg and Shinn (1964), Schlager (1981), and Neumann and Macintyre (1985), and documented throughout the Bahamas platforms using thermal remote sensing by Purkis et al. (2014). This winter phenomenon has historically been termed the "inimical bank-water effect." Here, we adopt the same terminology. Like the GBB, analogous shallow water depths on LBB, along the southwestern coast of Florida and in the Persian/Arabian Gulf are likely to foster the formation of inimical waters in these globally dispersed environments.

The SLIM model emphasizes how the GBB whitings zone is episodically ventilated by normal marine waters from both the Florida Straits and Tongue of the Ocean (Figs. 3, 4). Based on remotely sensed parameters relevant to the carbonate system, our calculations of Ω_{arag} for waters composed of both on-platform and off-platform seawater chemistry (Figs. 5, 8) revealed that bank top waters were always likely to precipitate aragonite ($\Omega_{arag} > 2$, Morse et al. 1980, 2003) but exhibited significant spatial heterogeneity, with lower Ω_{arag} values in the nearshore lee of Andros Island (Figs. 8, 11). Although the absolute values differ, spatial trends in $\Omega_{ara.}$ are consistent with prior work indicating that reduced Ω_{arag} to the west of Andros Island resulted from depleted alkalinity in aged waters (Broecker and Takahashi 1966; Geyman et al. 2022). Differences in absolute values of $\Omega_{ara.}$ are likely driven by the resolution of our remotely sensed datasets, and our assumption of conservative behavior. In concert, these datasets highlight regions of high Ω_{arag} near the platform margin, which is frequently bathed by warmer waters from the Florida Straits in the winter months.

Hydrodynamic mixing occurring in the winter months on the platform top is estimated to have up to three times the capacity to raise $\Omega_{ara.}$ than summer mixing (note steeper winter slopes in Fig. 5). Hence, in the case of the whitings zone, winter mixing of warm off-platform waters with cold on-platform waters amplifies $\Omega_{ara.}$ to a much greater degree that can be achieved in summer. Establishment of large temperature differentials between on-platform and off-platform water masses in the winter correspond to differences in Ω_{arag} of up to 0.4 (Fig. 5), which has implications for carbonate precipitation rates. Carbonate precipitation rate (R) is known to be exponentially related to Ω_{arag}, such that $R = k_p(\mathrm{W} - 1)^n$, where n is the empirical reaction order and k_p is the precipitation rate constant (Morse 1986; Walter and Hanor 1979; Kier 1980; Mucci 1986; Morse et al. 2003). Values of k_p and n have been reported to vary between 0.102 and 0.417 mmole mg^{-1} hr^{-1}, and between 2.0 and 3.7, respectively (Broecker and Takahashi 1966; Morse et al. 1984, 2003; Morse 1986), so that a change in Ω_{arag} produces nonlinear variations in predicted precipitation rate. This seasonality of the amplification driven by changes in temperature differential, Ω_{arag} and consequent R, corresponds excellently to the seasonality of whitings frequency (Fig. 11). When the temperature differential is greatest, whitings are at their maximum frequency (Fig. 11B). As the temperature differential decreases through March and April to a minimum in July and August, whitings frequency follows in step. The correlation persists as the temperature differential

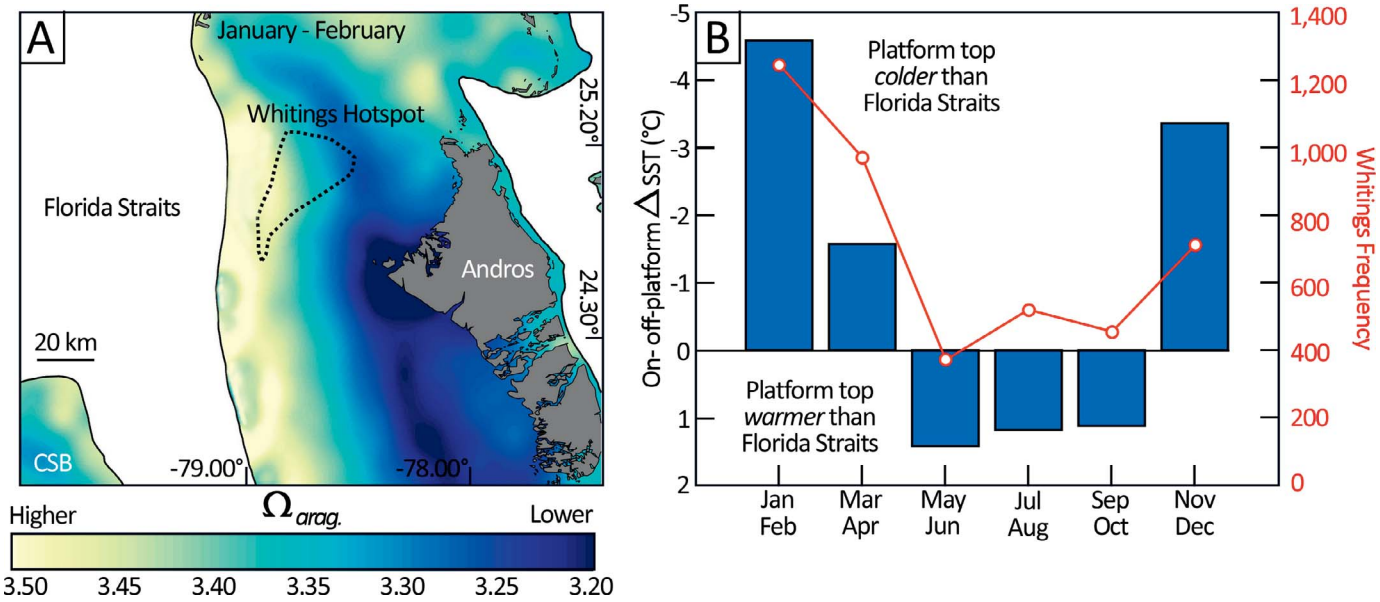

FIG. 11.—**A)** Map of the average degree of aragonite saturation (Ω_{arag}) on Great Bahama Bank (GBB) for the months of Jan and Feb 2016. Note the higher degree of spatial heterogeneity in Ω_{arag}, and the location of the whitings hotspot to the relatively increased Ω_{arag} values near the margin of GBB. **B)** Relationship between the differential in sea-surface temperature (ΔSST) between on- and off-platform waters and whitings frequency for bimonthly pairs in 2016. In winter, ΔSST is high (because the platform top is colder than the Florida Straits) and whitings are more frequent.

increases again through the late summer, fall, and into the winter, accompanied by an increase in whitings.

Data assembled by this study and the others which use remote sensing to monitor whitings cannot preclude the possibility that carbonate precipitation is happening apace during the summer (as would be predicted by high Ω_{arag}), but that the precipitation is not spatially confined as whitings that can be resolved from orbit. Three threads suggest that this is not the case. First, Shinn et al. (1989) measured the suspended-particulate concentrations inside summer whitings and in the clear water outside them, finding the former to be ten times higher than the latter. Second, even if the summer precipitation is spatially diffuse, it might reasonably be expected that it would have at least a subtle expression in satellite data, but none is seen. Finally, Robbins et al. (1997) elegantly develop the case that the carbonate produced by the whitings which are visible from orbit can easily account for all the lime mud atop the GBB and more besides. If abundant precipitation is ongoing unseen, it raises the question as to where this material is being deposited.

The spatial distribution of whitings further speaks to the interplay between hydrodynamics, temperature differentials, and water chemistry on GBB. Summer whitings are three times more frequent in the GBB precinct situated north of William's Island than south of it ($p < 0.05$, Table 2). Winter whitings behave similarly but are > 30% more frequent (Fig. 10A, $p = 0.535$, Table 2). Whitings are also significantly larger ($p < 0.05$, Table 2) in the southern precinct for both winter and summer months (Fig. 10B). As emphasized by the SLIM model, an important difference in the platform-top waters inhabiting the northern versus southern precincts is the degree to which they are mixed with off-platform waters. Mixing is enhanced in the northern precinct because tidal currents carry open-marine waters onto the platform and into the whitings zone from both the Florida Straits and, around the northern tip of Andros Island, also from Tongue of the Ocean (Figs. 3, 4). In contrast, the southern precinct does not receive the same flux of water from the Tongue of the Ocean, and, as discussed by Purkis et al. (2017), the rate of water transport across the margin is reduced by the hydrodynamic shadow cast by Cay Sal Bank (Fig. 4). As would be expected by the reduced rates of mixing, the frequency of whitings in the southern precinct is lower and their sizes are smaller (Fig. 10, Table 2).

Implications for Spatial Heterogeneity in Platform-Top Mud Production

Perhaps the most intriguing aspect of whitings mud production on GBB is that it does not occur equally across the bank, but rather is focused in an exceedingly limited area. The 15,000 whitings counted in 2012, 2014, and 2016 were restricted to < 10% of the area of GBB, and > 35% of the total occur in < 1% of that area (the peak whitings zone, Fig. 1B). It follows, therefore, that lime mud generated by whitings should not be equally distributed over the platform. The GBB facies maps produced by Harris et al. (2015), which was exhaustively ground-truthed by samples collected by Reijmer et al. (2009), show tight correspondence between the locus of production of whitings mud and the occurrence of muddy facies—see Figure 8 in Purkis et al. (2019b). Similar restrictions in various whitings "hotspots" were also observed atop LBB (Lloyd 2012) and in the Persian/Arabian Gulf (Shanableh et al. 2019) suggesting that localization of peak whitings zones may not be unique to GBB. The implication here is that prevailing platform-top currents are either too weak to move the mud much beyond the zone of its production, or that the currents beyond this zone are sufficiently swift to winnow away any transported mud. The SLIM model suggests that both realities are at play across the 100,000 sq. km GBB, depending on location.

Variability in the strength and location of the interaction of on- and off-platform water masses has the potential to drive significant spatial heterogeneity in the locus and intensity of whitings formation. For example, although there is a consistent "peak whitings" zone observed in all three years mapped in this study, we note variability in the monthly distribution of whitings across the platform top. A secondary whitings hotspot is observed during some months of the year to the west of the tidal outflows that separate Big Wood Cay and Mangrove Cay in the southern half of Andros Island (Fig. 1B). Dynamic changes in the strength, orientation, or temperature of the on- and off-platform water masses are expected to shift the location and intensity of whitings formation through time. For GBB, such changes may be autogenic (*per* Purkis et al. 2016), else allogenic, including variations in the strength and position of the Gulf Stream (McCarthy et al. 2012; Sallenger et al. 2012; Ezer et al. 2013; Smeed et al. 2014; Wdowinski et al. 2016; Caesar et al. 2018; Ezer 2019)

as induced, for instance, by the El Niño Southern Oscillation, the North Atlantic Oscillation, the Atlantic Meridional Overturning Circulation, and sea-level change. In addition, these atmospheric and oceanographic drivers could also be predicted to influence the temperature differential of on- and off-platform water masses, which in turn will impact the spatial distribution of Ω_{arag}, carbonate precipitation rate (R), and consequently, the propensity for enhanced whitings formation. The geological implication of the whitings factory waxing and waning, and also their migration across the platform, will be stratigraphic heterogeneity. In the case of the GBB, this results in a complex interweaving of grainy and muddy sediments. Turpin et al. (2011) illustrate this excellently, emphasizing how the Miocene GBB's ramp morphology was particularly conducive to whitings. Analyzing the geochemical variation of the Miocene lime muds and their aragonite-needle morphology, Turpin et al. suggest that whitings were the dominant mechanism for copious Miocene mud production. Geyman et al. (2022) advocate for reduced Miocene carbonate mud production, later in the Miocene than the period considered by Turpin et al. (2011), by virtue of a decreased supply of high-alkalinity water to the tropical Atlantic because of reduced Mediterranean outflow at that time.

Big and Inimical Platforms Have Few Reefs but Many Whitings

This article highlights the interplay between hydrodynamics and seawater chemistry as a precondition for enhanced formation of larger whitings. Underlying this interplay is the importance of pronounced winter temperature differentials between on- and off-platform waters; the inimical bank-water effect. This effect, on the face of it, might be considered an inconsequential meteorological quirk. However, it holds the potential to have a drastic bearing on the style of carbonate-platform development, suppressing the development of platform-edge reefs (Schlager 1981; Neumann and Macintyre 1985; Purkis et al. 2014) and triggering the prodigious production of lime mud in the platform interior via whitings. This effect might reasonably explain the prominence of non-reef rimmed flat-topped modern carbonate platforms in the Atlantic trade-wind belt, a morphology rarely observed in the tropical Pacific and Indian oceans, where reef-rimmed platforms dominate.

The production of chilled winter bank waters is tied to platform size, as can be emphasized by a map of the average winter temperature anomaly between on- and off-platform waters for the banks of the Bahamas (Fig. 12). This anomaly map was created by subtracting the SST values for each platform-top pixel from the average temperature of the off-platform waters situated within a 15 km buffer surrounding each platform. Daily anomalies were computed, and Figure 12 captures the average of these across the six winter months (Nov–Apr) for the 2012 through 2016 time period considered by this paper. As reported by Purkis et al. (2014) and further emphasized by this winter-anomaly map, of all the Bahamian platforms, only the two largest—Great and Little Bahama Bank (100,000 sq. km and 17,000 in area, respectively) develop widespread inimical winter platform-top waters. Platforms smaller than 6,000 sq. km do not because the bank-top waters have a short residence time. Accordingly, the Great and Little Bahama Banks host abundant whitings. The Caicos Platform, which has an area of 6,200 sq. km, anecdotally hosts whitings, but none could be identified through careful inspection of the daily 2012, 2014, and 2016 MODIS archives, indicating that Caicos whitings are below the detection limits of MODIS imagery, and, at best, ephemeral. Cay Sal Bank, which is 5,200 sq. km in area, lacks whitings, as do the smaller Crooked Acklins and Cat Island platforms (2,600 sq. km and 1,700 sq. km, respectively). With a maximum offset of 100 km between these localities, it would be a stretch to ascribe their propensities for whitings to regional differences in ocean chemistry. Instead, the data emphasize 6,000 sq. km as a minimum platform area that a Bahamian-type platform must attain in order to initiate a whitings mud factory driven by winter temperature differentials. As explored in the following section, meteorological control of the morphology of modern platforms and their facies successions might carry important lessons for the geological record. This control might plausibly be restricted to the trade-wind belt, however, where the chilling effect of winter cold fronts is acute.

Implications for the Distribution of Whitings in the Geological Record

Implicating the formation of inimical waters in the enhanced production of whitings further constrains likely environmental conditions conducive to mud deposition in the geological record. There are at least three key sedimentological and geochemical lessons provided by the GBB whitings for understanding mud distribution on analogous platforms in the geological record. First, and as emphasized by Robbins et al. (1997), the rates of production are exceedingly high. Large packages of lime mud have been observed throughout Earth history, including the Holocene fine-grained aragonite deposits atop GBB (Cloud 1962; Reijmer et al. 2009; Harris et al. 2015; Purkis and Harris 2016; Lopez-Gamundi et al. 2022) as well as those that were deposited as peri-platform sediments on the slopes of GBB in the relatively recent past (Droxler et al. 1983; Droxler and Schlager 1985; Eberli and Ginsburg 1989; Eberli et al. 1997; Anselmetti et al. 2000; Malone 2000; Rendle-Bühring and Reijmer 2005) and in the Miocene (Turpin et al. 2011) and the Pliocene (Reuning et al. 2006). Copious quantities of mud associated with microbial formation mechanisms have been described in Mesozoic sections around the globe (Jenkyns 1980; Sandberg 1985; Arthur et al. 1988; Kazmierczak et al. 1994), and thick sequences of carbonate mudstones are observed in the Neoproterozoic record (Hoffman et al. 1998; Hoffman and Schrag 2002). The mud factory has certainly been productive in a range of environmental settings throughout geological time. Second, whitings mud may not be widely redistributed beyond the area in which it is produced (Purkis et al. 2019b), suggesting that ancient mud deposits spanning great distances may reflect a variable hydrodynamic setting that not only traversed the platform top, but changed in location and intensity through time. And third, in the Modern at least, the whitings mud factory is temperamental, requiring a nuanced interaction between SST, ocean chemistry, and hydrodynamics, which can work together to amplify the rate of whitings production, whether by physical, chemical, or biological processes—the "Goldilocks" combination of factors proposed by Purkis et al. (2017).

The observation that hydrodynamic mixing of temperature-differentiated water masses can create conditions favorable for enhanced whitings formation has significant implications for understanding rates and loci of lime-mud production in the geological record. Although the results of this study and others (e.g., Lloyd 2012; Long 2016; Purkis et al. 2017; Shanableh et al. 2019; Yao et al. 2023) document enhanced winter whitings, summer whitings are also observed in all these depositional environments when temperature differentials are minimal. We suggest that several mechanisms may coexist through time which can generate whitings. Understanding the dynamic balance between these mechanisms is important to decipher the geochemical signatures that whitings record. For instance, if whitings are in fact abraded and resuspended material, their chemical and isotopic signatures record the cumulation of environmental signals, vital fractionation effects, and traces of the environment of original grain deposition (Trower et al. 2019; Geyman et al. 2022). Alternatively, if whitings are water-column precipitates, their chemical and isotopic composition likely represents a snapshot in geological time of ambient water chemistry, but impacts of vital effects produced by biological activity should not be ruled out. Consequently, constraining the degree and direction of the hydrodynamic influence on the size and formation rate of whitings, while environmental conditions evolved, will provide insight into the significance of the biogeochemical records stored in carbonate muds through geological time. It is important to clarify that these postulations are based on observations of a modern system, but they may provide a testable

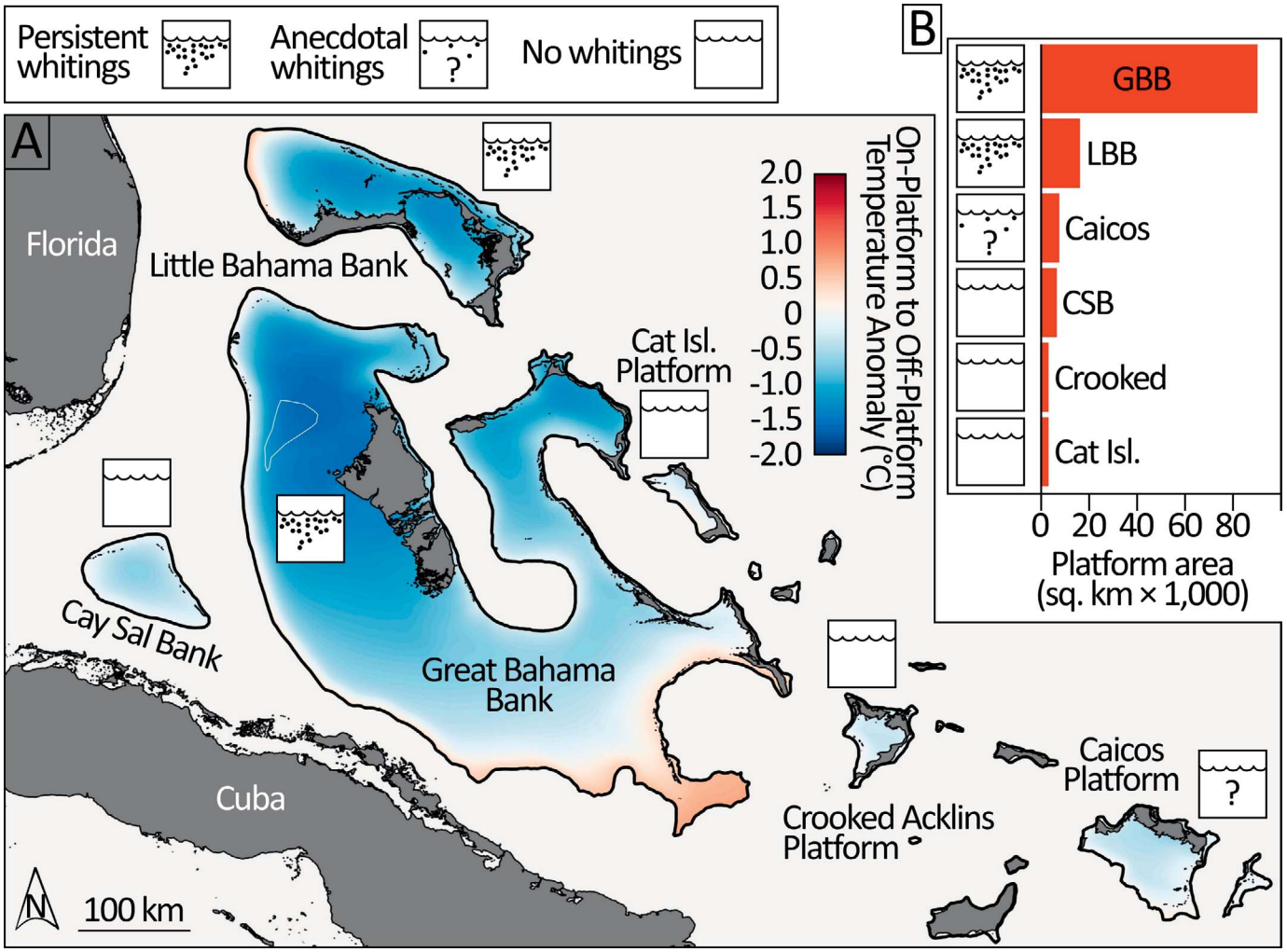

FIG. 12.—**A)** Map of the average winter (Nov–Apr) temperature anomaly between on- and off-platform waters for the Bahamas platforms for the period 2012 through 2016 derived from analysis of GHRSST L4 Global Foundation sea-surface-temperature data (Chao et al. 2009). A positive anomaly (red in the color ramp) corresponds to the situation where the off-platform waters are cooler than those on the platform top. A negative anomaly (blue) occurs when the on-platform waters are colder than those off the platform. Note that the whitings zone on the Great Bahama Bank (GBB) (white polygon) is situated in the zone of maximum negative anomaly. Little Bahama Bank (LBB), which also hosts abundant whitings, develops a similarly pronounced winter temperature anomaly. **B)** Charts the area of each of the Bahamian platforms. Only the two largest, GBB and LBB, host whitings which can be resolved from orbit.

framework for interpreting the elemental and isotopic composition of lime mud in the rock record.

CONCLUSIONS

New data assembled in this study confirm that wintertime GBB whitings are more prevalent and larger than those in the summer. This result is in opposition to thermodynamic expectations and emphasizes an alternative suite of environmental, hydrodynamic, and geochemical forcings that localize whitings lime-mud production atop GBB. Our simulation of hydrodynamics on and around the platform, combined with modeling of Ω_{arag}, suggests that the formation of inimical bank-top waters is key to amplifying the winter whitings factory. This seasonal temperature disparity explains why whitings in the Modern are apparently restricted to the subtropics and trade-wind belt. The intensity of the trigger afforded by inimical waters is plausibly related to platform size and might have profound implications for the sedimentology of platforms where it exists. For instance, because of the copious quantities of aragonitic mud that the whitings factory can generate, the Modern platforms on which it exists tend to be expansive and flat-topped. We hope that our work will provoke further examination of the varying controls of skeletal and precipitated carbonate grains in the modern and ancient alike.

SUPPLEMENTAL MATERIAL

Supplemental material is available from the SEPM Data Archive: https://www.sepm.org/supplemental-materials.

ACKNOWLEDGMENTS

Gratitude to Liisa Rohtla, Dietrich Kuhlmann, and Matthew Aldrich for their assistance counting whitings. Discussion with Peter Swart, Gregor Eberli, and Ceci Lopez-Gamundi is always fertile. We further extend our thanks to the CSL Center for Carbonate Research in the Department of Marine Geosciences, University of Miami, who have supported us. Computational resources were provided by the Consortium des Équipements de Calcul Intensif (CÉCI), funded by the F.R.S.-FNRS under Grant No. 2.5020.11. We are especially grateful to Ethan Grossman and an anonymous reviewer for

their constructive critique. While accomplishing this work, Thomas Dobbelaere was a Ph.D. student funded by a grant of the Fonds Spéciaux de Recherche (FSR) of UC Louvain.

REFERENCES

Anselmetti, F.S., Eberli, G.P., and Ding, Z.D., 2000, From the Great Bahama Bank into the Straits of Florida: a margin architecture controlled by sea-level fluctuations and ocean currents: Geological Society of America, Bulletin, v. 112, p. 829–844.

Arthur, M.A., Dean, W.E., and Pratt, L.M., 1988, Geochemical and climatic effects of increased marine organic carbon burial at the Cenomanian–Turonian boundary: Nature, v. 335(6192), p. 714–717.

Bethke, C., and Yeakel, S., 2018, Geochemist's Workbench: RockWare, Inc., Reference Manual, Release 12.0.

Black, M., 1933, The precipitation of calcium carbonate on the Great Bahama Bank: Geological Magazine, v. 70, p. 455–466.

Boss, S.K., and Neumann, A.C., 1993, Physical versus chemical processes of "whiting" formation in the Bahamas: Carbonates and Evaporites, v. 8, p. 135–148.

Broecker, W.S., and Takahashi, T., 1966, Calcium carbonate precipitation on the Bahama Banks: Journal of Geophysical Research, v. 71, p. 1575–1602.

Broecker, W.S., Sanyal, A., and Takahashi, T., 2000, The origin of Bahamian whitings revisited: Geophysical Research Letters, v. 27, p. 3759–3760.

Bustos-Serrano, H., Morse, J.W., and Millero, F.J., 2009, The formation of whitings on the Little Bahama Bank: Marine Chemistry, v. 113, p. 1–8.

Caesar, L., Rahmstorf, S., Robinson, A., Feulner, G., and Saba, V., 2018, Observed fingerprint of a weakening Atlantic Ocean overturning circulation: Nature, v. 556(7700), p. 191.

Cai, W.-J., Hu, X., Huang, W.-J., Wang, Y., Peng, T.-H., and Zhang, X., 2010, Alkalinity distribution in the Western North Atlantic Ocean margins: Journal of Geophysical Research, Oceans, v. 115, no. C08014.

Chao, Y., Li, Z., Farrara, J.D., and Hung, P., 2009, Blending sea-surface temperatures from multiple satellites and *in situ* observations for coastal oceans: Journal of Atmospheric and Oceanic Technology, v. 26, p. 1415–1426.

Cloud, P.E., Jr., 1962, Environment of calcium carbonate deposition west of Andros Island, Bahamas: U.S. Geological Survey, Professional Paper 350, 138 p.

Cummings, J.A., 2005, Operational multivariate ocean data assimilation: Royal Meteorological Society A, Quarterly Journal, v. 131, p. 3583–3604.

Cummings, J.A., and Smedstad, O.M., 2013, Variational data assimilation for the global ocean, *in* Park, S.K., and Xu, L., eds., Data Assimilation for Atmospheric, Oceanic and Hydrologic Applications, Volume II: Berlin, Springer, p. 303–343.

Dierssen, H.M., Zimmerman, R.C., and Burdige, D.J., 2009, Optics and remote sensing of Bahamian carbonate sediment whitings and potential relationship to wind-driven Langmuir circulation: Biogeosciences, v. 6, p. 487–500.

Drever, J.I., 1988, The Geochemistry of Natural Waters: 2nd Edition: Englewood Cliffs, Prentice Hall, 600 p.

Droxler, A.W., and Schlager, W., 1985, Glacial versus interglacial sedimentation rates and turbidite frequency in the Bahamas: Geology, v. 13, p. 799–802.

Droxler, A.W., Schlager, W., and Whallon, C.C., 1983, Quaternary aragonite cycles and oxygen-isotope record in Bahamian carbonate ooze: Geology, v. 11, p. 235–239.

Eberli, G.P., and Ginsburg, R.N., 1989, Cenozoic progradation of northwestern Great Bahama Bank, a record of lateral platform growth and sea-level fluctuations, *in* Crevello, P.D., Wilson, J.L., Sarg, J.F., and Read, J.F., eds., Controls on Carbonate Platform and Basin Development: SEPM, Special Publication 44, p. 339–351.

Eberli, G.P., Swart, P.K., McNeill, D.F., Kenter, J.A.M., Anselmetti, F.S., Melim, L.A., and Ginsburg, R.N., 1997, A synopsis of the Bahamas Drilling Project: results from two deep core borings drilled on the Great Bahama Bank: Proceedings of the Ocean Drilling Program, Initial Reports, v. 166, p. 23–41.

Egbert, G.D., and Erofeeva, S.Y., 2002, Efficient inverse modeling of barotropic ocean tides: Journal of Atmospheric and Oceanic Technology, v. 19, p. 183–204.

Enos, P., 1974, Map of Surface Sediment Facies of the Florida–Bahamas Plateau: Geological Society of America.

Ezer, T., 2019, Numerical modeling of the impact of hurricanes on ocean dynamics: Sensitivity of the Gulf Stream response to storm's track: Ocean Dynamics, v. 69, p. 1053–1066.

Ezer, T., Atkinson, L.P., Corlett, W.B., and Blanco, J.L., 2013, Gulf Stream's induced sea level rise and variability along the US mid-Atlantic coast: Journal of Geophysical Research, Oceans, v. 118, p. 685–697.

Figueiredo, J., Thomas, C.J., Deleersnijder, E., Lambrechts, J., Baird, A.H., Connolly, S.R., and Hanert, E., 2022, Global warming decreases connectivity among coral populations: Nature Climate Change, v. 12, p. 83–87.

Fox, D.N., Teague, W.J., Barron, C.N., Carnes, M.R., and Lee, C.M., 2002, The modular ocean data assimilation system (MODAS): Journal of Atmospheric and Oceanic Technology, v. 19, p. 240–252.

Frys, C., Saint-Amand, A., Le Hénaff, M., Figueiredo, J., Kuba, A., Walker, B., Lambrechts, J., Vallaeys, V., Vincent, D., and Hanert, E., 2020, Fine-scale coral connectivity pathways in the Florida Reef Tract: implications for conservation and restoration: Frontiers in Marine Science, v. 7, p. 312–317.

Geyman, E.C., and Maloof, A.C., 2019, A diurnal carbon engine explains ^{13}C-enriched carbonates without increasing the global production of oxygen: National Academy of Sciences [USA], Proceedings, v. 116, p. 24,433–24,439.

Geyman, E.C., Wu, Z., Nadeau, M.D., Edmonsond, S., Turner, A., Purkis, S.J., Howes, B., Dyer, B., Ahm, A.S.C., Yao, N., and Deutsch, C.A., 2022. The origin of carbonate mud and implications for global climate: National Academy of Sciences [USA], Proceedings, v. 119, no. 2210617119.

Ginsburg, R.N., and Shinn, E.A., 1964, Distribution of the reef-building community in Florida and the Bahamas: American Association of Petroleum Geologists, Bulletin, v. 48, p. 527–527.

Gledhill, D.K., Wanninkhof, R., Millero, F.J., and Eakin, M., 2008, Ocean acidification of the greater Caribbean region 1996–2006: Journal of Geophysical Research, Oceans, v. 113(C10), p. 1–11.

Granier, B., 2012, The contribution of calcareous green algae to the production of limestones: a review: Geodiversitas, v. 34, p. 35–60.

Grech, A., Hanert, E., McKenzie, L., Rasheed, M., Thomas, C., Tol, S., Wang, M., Waycott, M., Wolter, J., and Coles, R., 2018, Predicting the cumulative effect of multiple disturbances on seagrass connectivity: Global Change Biology, v. 24, p. 3093–3104.

Hanert, E., Legat, V., and Deleersnijder, É., 2003, A comparison of three finite elements to solve the linear shallow water equations: Ocean Modelling, v. 5, p. 17–35.

Hanert, E., Le Roux, D.Y., Legat, V., and Deleersnijder, E., 2005, An efficient Eulerian finite element method for the shallow water equations: Ocean Modelling, v. 10, p. 115–136.

Harris, P.M., Purkis, S.J., Ellis, J., Swart, P.K., and Reijmer, J.J., 2015, Mapping bathymetry and depositional facies on Great Bahama Bank: Sedimentology, v. 62, p. 566–589.

Hjulström, F., 1935, Studies of the morphological activity of rivers as illustrated by the River Fyris [Ph.D. Thesis]: The Geological Institution, University of Upsala, 250 p.

Hoffman, P.F., and Schrag, D.P., 2002, The snowball Earth hypothesis: testing the limits of global change: Terra Nova, v. 14, p. 129–155.

Hoffman, P.F., Kaufman, A.J., Halverson, G.P., and Schrag, D.P., 1998, A Neoproterozoic snowball Earth: Science: v. 281, p. 1342–1346.

Jenkyns, H.C., 1980, Cretaceous anoxic events: from continents to oceans: Geological Society of London, Journal, v. 137, p. 171–188.

Kaczmarek, S.E., Hicks, M.K., Fullmer, S.M., Steffen, K.L., and Bachtel, S.L., 2010, Mapping facies distributions on modern carbonate platforms through integration of multispectral Landsat data, statistics-based unsupervised classifications, and surface sediment data: American Association of Petroleum Geologists, Bulletin, v. 94, p. 1581–1606.

Kazmierczak, J., Gruszczynski, M., Coleman, M.L., and Kempe, S., 1994, Coccoid cyanobacterial origin of common micritic and peloidal limestones: Jurassic and Modern examples [Abstract]: 14th International Sedimentological Congress, Abstracts, p. B-6.

Kier, R.S., 1980, The dissolution kinetic of biogenic calcium carbonates in seawater: Geochimica et Cosmochimica Acta, v. 44, p. 241–252.

Knoll, A.H., and Swett, K., 1990, Carbonate deposition during the late Proterozoic Era: an example from Spitsbergen: American Journal of Science, v. 290, p. 104–132.

Larson, E.B., and Mylroie, J.E., 2014, A review of whiting formation in the Bahamas and new models: Carbonates and Evaporites, v. 29, p. 337–347.

Le Bars, Y., Vallaeys, V., Deleersnijder, É., Hanert, E., Carrere, L., and Channelière, C., 2016, Unstructured-mesh modeling of the Congo river-to-sea continuum: Ocean Dynamics, v. 66, p. 589–603.

Li, Y., Wolanski, E., Dai, Z., Lambrechts, J., Tang, C., and Zhang, H., 2018, Trapping of plastics in semi-enclosed seas: insights from the Bohai Sea, China: Marine Pollution Bulletin, v. 137, p. 509–517.

Lisle, J.T., and Robbins, L.L., 2016, Viral lysis of photosynthesizing microbes as a mechanism for calcium carbonate nucleation in seawater: Frontiers in Microbiology, v. 7, p. 1–7.

Lloyd, R.A., 2012, Remote sensing of whitings in the Bahamas [M.Sc. Thesis]: University of South Florida, p. 120.

Long, J., Hu, C., and Robbins, L., 2014, Whiting events in SW Florida coastal waters: a case study using MODIS medium-resolution data: Remote Sensing Letters, v. 5, p. 539–547.

Long, J.S., 2016, Whiting Events Off Southwest Florida: Remote Sensing and Field Observations [Ph.D. Thesis]: University of South Florida, p. 322.

Lopez-Gamundi, C., Dobbelaere, T., Hanert, E., Harris, P.M., Eberli, G., and Purkis, S.J., 2022, Simulating sedimentation on the Great Bahama Bank: sources, sinks and storms: Sedimentology, v. 69, p. 2,693–2,714.

Malone, M., 2000, Data report: geochemistry and mineralogy of periplatform carbonate sediments: sites 1006, 1008, and 1009: Proceedings of the Ocean Drilling Program, Scientific Results, v. 166, p. 145–152.

McCarthy, G., Frajka-Williams, E., Johns, W.E., Baringer, M.O., Meinen, C.S., Bryden, H.L., Rayner, D., Duchez, A., Roberts, C., and Cunningham, S.A., 2012, Observed interannual variability of the Atlantic meridional overturning circulation at 26.5° N: Geophysical Research Letters, v. 39, p. 1–5.

Morse, J.W., 1986, The surface chemistry of calcium carbonate minerals in natural waters: an overview: Marine Chemistry, v. 20, p. 91–112.

Morse, J.W., Mucci, A., and Millero, F.J., 1980, The solubility of calcite and aragonite in seawater of 35%, salinity at 25 °C and atmospheric pressure: Geochimica et Cosmochimica Acta, v. 44, p. 85–94.

Morse, J.W., Millero, F.J., Thurmond, V., Brown, E., and Ostlund, H.G., 1984, The carbonate chemistry of Grand Bahama Bank waters: after 18 years another look: Journal of Geophysical Research, Oceans, v. 89, p. 3604–3614.

Morse, J.W., Gledhill, D.K., and Millero, F.J., 2003, $CaCO_3$ precipitation kinetics in waters from the Great Bahama Bank: implications for the relationship between bank hydrochemistry and whitings: Geochimica et Cosmochimica Acta, v. 67, p. 2819–2826.

Mucci, A., 1986, Growth kinetics and composition of magnesian calcite overgrowths precipitated from seawater: quantitative influence of orthophosphate ions: Geochimica et Cosmochimica Acta, v. 50, p. 2255–2265.

Neumann, A.C., and Macintyre, I.G., 1985, Reef response to sea level rise: keep-up, catch-up or give-up: Fifth International Coral Reef Congress, Proceedings, Tahiti, p. 105–110.

Neumann, A.C., Gebelein, C.D., and Scoffin, T.P., 1970, The composition, structure, and erodibility of subtidal mats, Abaco, Bahamas: Journal of Sedimentary Petrology, v. 40, p. 274–297.

Purkis, S.J., and Harris, P.M., 2016, The extent and patterns of sediment filling of accommodation space on Great Bahama Bank: Journal of Sedimentary Research, v. 86, p. 294–310.

Purkis, S., Kerr, J., Dempsey, A., Calhoun, A., Metsamaa, L., Riegl, B., Kourafalou, V., Bruckner, A., and Renaud, P., 2014, Large-scale carbonate platform development of Cay Sal Bank, Bahamas, and implications for associated reef geomorphology: Geomorphology, v. 222, p. 25–38.

Purkis, S.J., van de Koppel, J., and Burgess, P.M., 2016, Spatial self-organization in carbonate depositional environments, *in* Budd, D.A., Hajek, E.A., and Purkis, S.J., eds., Autogenic Dynamics and Self-Organization in Sedimentary Systems: SEPM, Special Publication 106, p. 53–66.

Purkis, S., Cavalcante, G., Rohtla, L., Oehlert, A.M., Harris, P.M., and Swart, P.K., 2017, Hydrodynamic control of whitings on Great Bahama Bank: Geology, v. 45, p. 939–942.

Purkis, S.J., Gleason, A.C., Purkis, C.R., Dempsey, A.C., Renaud, P.G., Faisal, M., Saul, S., and Kerr, J.M., 2019a, High-resolution habitat and bathymetry maps for 65,000 sq. km of Earth's remotest coral reefs: Coral Reefs, v. 38, p. 467–488.

Purkis, S.J., Harris, P., and Cavalcante, G., 2019b, Controls of depositional facies patterns on a modern carbonate platform: insight from hydrodynamic modeling: The Depositional Record, v. 5, p. 421–437.

Reijmer, J.J., Swart, P.K., Bauch, T., Otto, R., Reuning, L., Roth, S., and Zechel, S., 2009, A re-evaluation of facies on Great Bahama Bank I: new facies maps of western Great Bahama Bank, *in* Swart, P.K., Eberli, G.P., and McKenzie, J.A., eds., Perspectives in Carbonate Geology: A Tribute to the Career of Robert Nathan Ginsburg: International Association of Sedimentologists, Special Publication 41, p. 29–46.

Rendle-Bühring, R.H., and Reijmer, J.J., 2005, Controls on grain-size patterns in periplatform carbonates: marginal setting versus glacio-eustacy: Sedimentary Geology, v. 175, p. 99–113.

Reuning, L., Reijmer, J.J., Betzler, C., Timmermann, A., and Steph, S., 2006, Sub-Milankovitch cycles in periplatform carbonates from the Early Pliocene Great Bahama Bank: Paleoceanography, v. 21, p. 1–11.

Riding, R., 1991, Classification of microbial carbonates, *in* Riding R., ed., Calcareous Algae and Stromatolites, Springer, p. 21–51.

Riding, R., 2006, Cyanobacterial calcification, carbon dioxide concentrating mechanisms, and Proterozoic–Cambrian changes in atmospheric composition: Geobiology, v. 4, p. 299–316.

Robbins, L.L., and Blackwelder, P.L., 1992, Biochemical and ultrastructural evidence for the origin of whitings: a biologically induced calcium carbonate precipitation mechanism: Geology, v. 20, p. 464–468.

Robbins, L.L., Tao, Y., and Evans, C.A., 1997, Temporal and spatial distribution of whitings on Great Bahama Bank and a new lime mud budget: Geology, v. 25, p. 947–950.

Robinson, R.A., and Stokes, R.H., 1968, Electrolyte Solutions: London, Butterworths, 571 p.

Rosón, G., Ríos, A.F., Pérez, F.F., Lavín, A., and Bryden, H.L., 2003, Carbon distribution, fluxes, and budgets in the subtropical North Atlantic Ocean (24.5° N): Journal of Geophysical Research, Oceans, v. 108(C5).

Sallenger, A.H., Jr., Doran, K.S., and Howd, P.A., 2012, Hotspot of accelerated sea-level rise on the Atlantic coast of North America: Nature Climate Change, v. 2, p. 884.

Sandberg, P.A., 1983, An oscillating trend in Phanerozoic non-skeletal carbonate mineralogy: Nature, v. 305(5929), p. 19.

Sandberg, P.A., 1985, Nonskeletal aragonite and pCO_2 in the Phanerozoic and Proterozoic: Geophysical Monograph Series, v. 32, p. 585–594.

Schlager, W., 1981, The paradox of drowned reefs and carbonate platforms: Geological Society of America, Bulletin, v. 92, p. 197–211.

Schultze-Lam, S., Schultze-Lam, S., Beveridge, T.J., and Des Marais, D.J., 1997, Whiting events: biogenic origin due to the photosynthetic activity of cyanobacterial picoplankton: Limnology and Oceanography, v. 42, p. 133–141.

Schuster, U., McKinley, G.A., Bates, N., Chevallier, F., Doney, S.C., Fay, A.R., González-Dávila, M., Gruber, N., Jones, S., Krijnen, J., and Landschützer, P., 2013, An assessment of the Atlantic and Arctic sea–air CO_2 fluxes, 1990–2009: Biogeosciences, v. 10, p. 607–627.

Shanableh, A., Al-Ruzouq, R., Gibril, M.B.A., Flesia, C., and AL-Mansoori, S., 2019, Spatiotemporal mapping and monitoring of whiting in the semi-enclosed Gulf using Moderate Resolution Imaging Spectroradiometer (MODIS) time series images and a generic ensemble tree-based model: Remote Sensing, v. 11, p. 1–21.

Shinn, E.A., Steinen, R.P., Lidz, B.H., and Swart, P.K., 1989, Whitings, a sedimentologic dilemma: Journal of Sedimentary Petrology, v. 59, p. 147–161.

Smeed, D.A., McCarthy, G.D., Cunningham, S.A., Frajka-Williams, E., Rayner, D., Johns, W.E., Meinen, C.S., Baringer, M.O., Moat, B.I., Duchez, A., and Bryden, H.L., 2014, Observed decline of the Atlantic meridional overturning circulation 2004–2012: Ocean Science, v. 10, p. 29–38.

Smith, C.L., 1940, The Great Bahama Bank, I, general hydrographical and chemical features: Journal of Marine Research, v. 3, p. 147–170.

Swart, P.K., Oehlert, A.M., Mackenzie, G.J., Eberli, G.P., and Reijmer, J.J.G., 2014, The fertilization of the Bahamas by Saharan dust: a trigger for carbonate precipitation? Geology, v. 42, p. 671–674.

Tao, Y., 1994, Whitings on Great Bahama Bank: distribution in space and time using Space Shuttle photographs [MS Thesis] University of South Florida, 205 p.

Thomas, C.J., Lambrechts, J., Wolanski, E., Traag, V.A., Blondel, V.D., Deleersnijder, E., and Hanert, E., 2014, Numerical modelling and graph theory tools to study ecological connectivity in the Great Barrier Reef: Ecological Modelling, v. 272, p. 160–174.

Thompson, J.B., Schultze-Lam, S., Beveridge, T.J., and Des Marais, D.J., 1997, Whiting events: biogenic origin due to the photosynthetic activity of cyanobacterial picoplankton: Limnology and Oceanography v. 42, p. 133–141.

Trower, E.J., Lamb, M.P., and Fischer, W.W., 2019, The origin of carbonate mud: Geophysical Research Letters, v. 46, p. 2696–2703.

Turpin, M., Emmanuel, L., Reijmer, J.J., and Renard, M., 2011, Whiting-related sediment export along the Middle Miocene carbonate ramp of Great Bahama Bank: International Journal of Earth Sciences, v. 100, p. 1875–1893.

Vallaeys, V., Kärnä, T., Delandmeter, P., Lambrechts, J., Baptista, A.M., Deleersnijder, E., and Hanert, E., 2018, Discontinuous Galerkin modeling of the Columbia River's coupled estuary-plume dynamics: Ocean Modelling, v. 124, p. 111–124.

Walter, L.M., and Hanor, J.S., 1979, Effect of orthophosphate on the dissolution kinetics of biogenic magnesian calcites: Geochimica et Cosmochimica Acta, v. 43, p. 1377–1385.

Wanninkhof, R., Triñanes, J., Park, G.H., Gledhill, D., and Olsen, A., 2019, Large decadal changes in air-sea CO_2 fluxes in the Caribbean Sea: Journal of Geophysical Research, Oceans, v. 124, p. 6960–6982.

Wdowinski, S., Bray, R., Kirtman, B.P., and Wu, Z., 2016, Increasing flooding hazard in coastal communities due to rising sea level: case study of Miami Beach, Florida: Ocean and Coastal Management, v. 126, p. 1–8.

Woosley, R.J., Millero, F.J., and Wanninkhof, R., 2016, Rapid anthropogenic changes in CO_2 and pH in the Atlantic Ocean: 2003–2014: Global Biogeochemical Cycles, v. 30, p. 70–90.

Wu, M., Harris, P.M., Eberli, G., and Purkis, S.J., 2021, Sea-level, storms, and sedimentation: controls on the architecture of the Andros tidal flats (Great Bahama Bank): Sedimentary Geology, v. 420, p. 1–16.

Yao, Y., Hu, C., and Barnes, B.B., 2023, Mysterious increases of whiting events in the Bahama Banks: Remote Sensing of Environment, v. 285, p. 1–15.

Yates, K.K., and Robbins, L.L., 1998, Production of carbonate sediments by a unicellular green alga: American Mineralogist, v. 83, p. 1503–1509.

Yates, K.K., and Robbins, L.L., 2001, Microbial lime-mud production and its relation to climate change, *in* Gerhard, L.C., Harrison, W.E., and Hanson, B.M., eds., Geological Perspectives of Global Climate Change: American Association of Petroleum Geologists, Studies in Geology 47, p. 237–292.

Received 12 August 2022; accepted 6 January 2023.